



NAVAL POSTGRADUATE SCHOOL

MONTEREY, CALIFORNIA

THESIS

**DEPTH DERIVATION FROM THE WORLDVIEW-2
SATELLITE USING HYPERSPECTRAL IMAGERY**

by

Michael J. Loomis, Jr.

March 2009

Thesis Advisor:
Thesis Co-advisor:

Philip A. Durkee
Richard C. Olsen

Approved for public release; distribution is unlimited

THIS PAGE INTENTIONALLY LEFT BLANK

REPORT DOCUMENTATION PAGE			<i>Form Approved OMB No. 0704-0188</i>	
Public reporting burden for this collection of information is estimated to average 1 hour per response, including the time for reviewing instruction, searching existing data sources, gathering and maintaining the data needed, and completing and reviewing the collection of information. Send comments regarding this burden estimate or any other aspect of this collection of information, including suggestions for reducing this burden, to Washington headquarters Services, Directorate for Information Operations and Reports, 1215 Jefferson Davis Highway, Suite 1204, Arlington, VA 22202-4302, and to the Office of Management and Budget, Paperwork Reduction Project (0704-0188) Washington DC 20503.				
1. AGENCY USE ONLY (Leave blank)		2. REPORT DATE March 2009	3. REPORT TYPE AND DATES COVERED Master's Thesis	
4. TITLE AND SUBTITLE Depth Derivation from the Worldview-2 Satellite Using Hyperspectral Imagery			5. FUNDING NUMBERS	
6. AUTHOR(S) Michael Joseph Loomis, Jr.				
7. PERFORMING ORGANIZATION NAME(S) AND ADDRESS(ES) Naval Postgraduate School Monterey, CA 93943-5000			8. PERFORMING ORGANIZATION REPORT NUMBER	
9. SPONSORING /MONITORING AGENCY NAME(S) AND ADDRESS(ES) N/A			10. SPONSORING/MONITORING AGENCY REPORT NUMBER	
11. SUPPLEMENTARY NOTES The views expressed in this thesis are those of the author and do not reflect the official policy or position of the Department of Defense or the U.S. Government.				
12a. DISTRIBUTION / AVAILABILITY STATEMENT Approved for public release; distribution is unlimited			12b. DISTRIBUTION CODE	
13. ABSTRACT (maximum 200 words) <p>The Worldview-2 satellite, scheduled for launch in 2009, will have a multispectral sensor with several additional spectral bands not available on current multispectral sensors. This research investigates the use of the additional yellow spectral band to derive bathymetry. A hyperspectral image acquired from the AVIRIS sensor was used as a substitute image for the Worldview-2 multispectral sensor. The image was processed using the Stumpf et al. (2003) "ratio method" to determine bathymetry in a section of Kaneohe Bay, Hawaii. Depths acquired using the green/blue, yellow/green and yellow/blue ratios were compared to ground truth bathymetry derived from a digital nautical chart. The results indicate that using the Stumpf et al. (2003) algorithm with yellow/green and yellow/blue ratios improves the accuracy of derived depths compared to depths derived using the green/blue ratio, especially in shallow waters.</p>				
14. SUBJECT TERMS Remote sensing, hyperspectral, multispectral, bathymetry, Worldview-2, Quickbird			15. NUMBER OF PAGES 69	
			16. PRICE CODE	
17. SECURITY CLASSIFICATION OF REPORT Unclassified	18. SECURITY CLASSIFICATION OF THIS PAGE Unclassified	19. SECURITY CLASSIFICATION OF ABSTRACT Unclassified	20. LIMITATION OF ABSTRACT UU	

THIS PAGE INTENTIONALLY LEFT BLANK

Approved for public release; distribution is unlimited

**DEPTH DERIVATION FROM THE WORLDVIEW-2 SATELLITE USING
HYPERSPSCTRAL IMAGERY**

Michael J. Loomis, Jr.
Lieutenant Commander, United States Navy
B.S., Rowan University, 1996

Submitted in partial fulfillment of the
requirements for the degree of

**MASTER OF SCIENCE IN METEOROLOGY AND PHYSICAL
OCEANOGRAPHY**

from the

**NAVAL POSTGRADUATE SCHOOL
March 2009**

Author: Michael J. Loomis, Jr.

Approved by: Philip A. Durkee
Thesis Advisor

Richard C. Olsen
Co-Advisor

Philip A. Durkee
Chairman, Department of Meteorology

THIS PAGE INTENTIONALLY LEFT BLANK

ABSTRACT

The Worldview-2 satellite, scheduled for launch in 2009, will have a multispectral sensor with several additional spectral bands not available on current multispectral sensors. This research investigates the use of the additional yellow spectral band to derive bathymetry. A hyperspectral image acquired from the AVIRIS sensor was used as a substitute image for the Worldview-2 multispectral sensor. The image was processed using the Stumpf et al. (2003) “ratio method” to determine bathymetry in a section of Kaneohe Bay, Hawaii. Depths acquired using the green/blue, yellow/green and yellow/blue ratios were compared to ground truth bathymetry derived from a digital nautical chart. The results indicate that using the Stumpf et al. (2003) algorithm with yellow/green and yellow/blue ratios improves the accuracy of derived depths compared to depths derived using the green/blue ratio, especially in shallow waters.

THIS PAGE INTENTIONALLY LEFT BLANK

TABLE OF CONTENTS

I.	INTRODUCTION.....	1
II.	BACKGROUND	5
A.	RADIATIVE TRANSFER FUNDAMENTALS	5
B.	TEST SITE	6
C.	MULTISPECTRAL IMAGERY FROM QUICKBIRD	7
D.	HYPERSPPECTRAL IMAGERY FROM AVIRIS	8
E.	MULTISPECTRAL IMAGERY FROM WORLDVIEW-2	9
F.	BATHYMETRY DERIVATION FROM REMOTELY SENSED DATA	10
III.	METHODS	13
A.	METHODOLOGY OVERVIEW	13
B.	QUICKBIRD	15
C.	AVIRIS.....	18
1.	Calibration and Spatial Subsetting	18
2.	Conversion to Top-of-Atmosphere Reflectance	18
3.	Regions of Interest	19
4.	Supervised Classification.....	19
5.	Bathymetric Derivation	20
a.	<i>Green/blue Ratio</i>	<i>20</i>
b.	<i>Yellow/green Ratio</i>	<i>20</i>
c.	<i>Yellow/blue Ratio</i>	<i>21</i>
IV.	RESULTS	23
A.	BATHYMETRY USING THE GREEN/BLUE RATIO	23
B.	BATHYMETRY USING THE YELLOW/GREEN RATIO	25
C.	BATHYMETRY USING THE YELLOW/BLUE RATIO	27
D.	TRANSECTS	29
1.	Transect 1	30
2.	Transect 2	33
V.	DISCUSSION	39
VI.	CONCLUSION	43
	APPENDIX A: AVIRIS REGRESSIONS	45
	APPENDIX B: QUICKBIRD REGRESSION	49
	LIST OF REFERENCES.....	51
	INITIAL DISTRIBUTION LIST	53

THIS PAGE INTENTIONALLY LEFT BLANK

LIST OF FIGURES

Figure 1.	Sigbee sounding machine, circa 1882. The device winches a weighted wire to measure depth. From NOAA Picture Library (http://www.history.noaa.gov/ships/albatross5.html)2
Figure 2.	Visible portions of the electromagnetic spectrum (From University of Arkansas at Little Rock 2006).5
Figure 3.	Kaneohe Bay study area.....7
Figure 4.	Quickbird Satellite (from: http://www.digitalglobe.com/index.php/85/QuickBird)8
Figure 5.	AVIRIS instrument mounted on an ER-2 aircraft. (From: http://aviris.jpl.nasa.gov/html/aviris.overview.html)9
Figure 6.	Worldview-2 Satellite. (From http://www.digitalglobe.com/index.php/88/WorldView-2)10
Figure 7.	Supervised classified Quickbird image (left). Green is sand, brown is non-sand substrate, and blue is optically deep water. Quickbird reflectance image (right).....17
Figure 8.	Kaneohe Bay tides for 10:59 AM, HST (GMT-10).....18
Figure 9.	AVIRIS classified image (left) and AVIRIS reflectance image (right). On the classified image, green is sand, blue is optically deep water, brown is reef.19
Figure 10.	Quickbird classified image (left) and AVIRIS classified image (right). The brown reef-classified areas match well between the two images.20
Figure 11.	Kaneohe Bay tides for March 1, 2005 at 12:55 PM HST (GMT-10)21
Figure 12.	Quickbird Reef Classified Bathymetry from green/blue ratio (left); AVIRIS Reef Classified Bathymetry from green/blue ratio (right). Light colors represent deeper depths, darker colors represent shallower depths. The black regions are masked out.....24
Figure 13.	Digital nautical chart (left) showing ground truth bathymetry with AVIRIS reflectance image (right).25
Figure 14.	AVIRIS Bathymetry from yellow/green ratio. Dark regions represent shallow bathymetry, lighter regions represent deep bathymetry.26
Figure 15.	AVIRIS reef classified bathymetry using the yellow/blue ratio.28
Figure 16.	SHOALS bathymetry showing depth variability of the reef along a short portion of a survey line in the study area. Retrieved from the Hawaii Coastal Geology Group online at: (http://www.soest.hawaii.edu/coasts/data/oahu/shoals.html)30
Figure 17.	Transect Line 1. The AVIRIS reflectance image is on the left, the digital nautical chart used for ground truth is on the right. The referenced reef flat and reef crest areas are marked on the reflectance image. The transect runs from west (pixel 1) to east (pixel 156).31
Figure 18.	Transect 1 bathymetry. The error bars represent uncertainty in actual ground truth depth as depicted in Figure 16. Negative values are emergent.....32

Figure 19.	Transect 1 derived depth and ground truth depth correlations for each ratio tested.	33
Figure 20.	Transect Line 2. The AVIRIS reflectance image is on the left, the digital nautical chart used for ground truth is on the right. The transect runs from the northeast (pixel 1) to southeast (pixel 378).....	35
Figure 21.	Transect 2 bathymetry. The error bars represent uncertainty in actual ground truth depth as depicted in Figure 16. Negative values are emergent....	36
Figure 22.	Transect 2 derived depth and ground truth depth correlations for each ratio tested.	37
Figure 23.	Attenuation rate of light with depth as a function of wavelength. (From: http://oceanworld.tamu.edu/resources/ocng_textbook/chapter06)	40
Figure 24.	AVIRIS reef regression to calibrate relative bathymetry to absolute bathymetry using the green/blue ratio. Points represent ground truth points extracted from the digital nautical chart (y axis) and the value of the same point on the AVIRIS image derived from the blue/green ratio relative bathymetry regression (x axis).....	45
Figure 25.	AVIRIS reef regression to calibrate relative bathymetry to absolute bathymetry using the yellow/blue ratio. Points represent ground truth points extracted from the digital nautical chart (y axis) and the value of the same point on the AVIRIS image derived from the yellow/blue ratio relative bathymetry regression (x axis).....	46
Figure 26.	AVIRIS reef regression to calibrate relative bathymetry to absolute bathymetry using the yellow/green ratio. Points represent ground truth points extracted from the digital nautical chart (y axis) and the value of the same point on the AVIRIS image derived from the yellow/green ratio relative bathymetry regression (x axis).....	47
Figure 27.	Quickbird reef regression to calibrate relative bathymetry to absolute bathymetry using the green/blue ratio. Blue points represent ground truth points extracted from the digital nautical chart (y axis) and the value of the same point on the Quickbird image derived from the green/blue ratio relative bathymetry regression (x axis).....	49

LIST OF TABLES

Table 1.	AVIRIS bands used for image processing	14
----------	--	----

THIS PAGE INTENTIONALLY LEFT BLANK

ACKNOWLEDGMENTS

First, I would like to extend my sincere gratitude to Dr. Philip Durkee for his inspirational guidance as my advisor and professor. I also extend my thanks to Dr. Richard Olsen for providing the motivation for this thesis, and for his assistance and mentorship. LCDR Brian Rivenbark deserves special recognition for being a sounding board for ideas and frustrations, and his tireless help with the details. Angela Puetz was available to help, no matter how seemingly trivial the question and I thank her for generous donation of her time. Finally, my wife Jennifer and my children Evan and Jenna deserve very heartfelt thanks for their understanding and support throughout this process and my career.

THIS PAGE INTENTIONALLY LEFT BLANK

I. INTRODUCTION

“The fishermen working on that slope where they are in the habit of finding coral at 150 and 200 fathoms, and their lines not allowing soundings in greater depths, imagine that the bottom cannot be found, and call it in their exaggerated jargon a bottomless abyss, impossible to be sounded. This idea entertained by people of experience in marine matters, as well as by the simple fishers, appears to be absurd, and founded merely on the fact that nobody has yet cared to undertake the trouble and expense required for such soundings, which according to all appearances will never be made unless some Prince orders for that purpose special vessels with suitable instruments” (Marsigli, 1725).

Since man began sailing the seas, he has been interested in the depth of the water upon which he sailed. From the earliest days, soundings were acquired using a lead weight on the end of a rope or wire (Figure 1). Taking soundings in this manner is time-consuming and only acquires depth at a single point. Yet, until the advent of sonar this technique remained the most viable means of bathymetric mapping (NOAA, 2006).

Undersea warfare, an integral part of World War I, inspired vigorous research into new means to detect underwater objects. The discovery that sound waves bounce off of objects, including the bottom of the sea, led to the development of “fathometers”, the predecessor to modern sonar. As a means of bathymetric mapping, the advent of sonar rendered lead weight line sounding obsolete and sonar remains the primary method by which bathymetry is obtained today. Single beam sonar acquires depth at a single point, much like lead line sounding, but depths are acquired far more rapidly along a survey line. Multi-beam and sidescan sonar improve upon this technique by acquiring depths in a swath along a survey line, greatly improving the resolution of the resultant soundings. If the survey lines are sufficiently close, it is possible to completely map the bathymetry of the survey region (Kunzig, 2000).

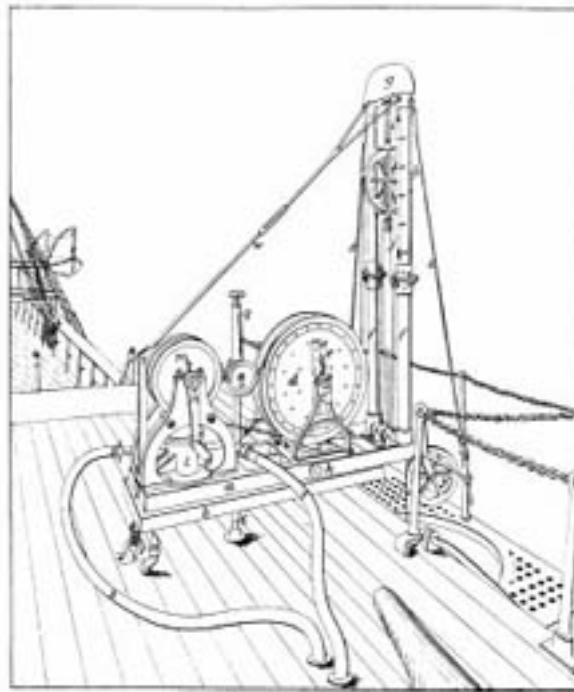


Figure 1. Sigbee sounding machine, circa 1882. The device winches a weighted wire to measure depth. From NOAA Picture Library (<http://www.history.noaa.gov/ships/albatross5.html>)

However, sonar-acquired bathymetry is still hampered by significant limitations. Ships are relatively slow and during a survey are restricted to even slower speeds, requiring a great deal of time to conduct a survey over even a limited area. Ships are limited by fuel and provisions and therefore are logistically restricted in how much surveying they can conduct at any one time. In a military sense, ships are unable to conduct soundings in a “denied area” or without coordinating permission from the country in which the territorial waters are located.

Remotely sensed bathymetry mapping is a relatively new manner by which many of the previous limitations are overcome. The variety of sensors and different techniques for processing imagery into bathymetry allows for a great deal of tailoring by the end-user to meet his specific needs. Remotely sensed bathymetry mapping is not without its own limitations though.

Generally speaking, two main branches of remotely sensed imagery are available for bathymetric mapping. Hyperspectral imagery, usually acquired from aircraft, measures the visible spectrum of many narrow spectral bands and generally has a spatial resolution on the order of a meter. Multispectral imagery, acquired from satellites, measures the visible spectrum in a few bands, typically with 2-20m spatial resolution. The advantages of airborne hyperspectral imagery are a narrower band resolution and higher spatial resolution. The advantages of hyperspectral imagery are offset by the logistics of requiring overflight by an aircraft to acquire the imagery. The logistics and expense of acquisition can become prohibitive in remote or denied areas (Mumby et al., 1999).

The advantage of satellite-acquired multispectral imagery is the ability to retrieve a great deal of imagery quickly with a short revisit time. Multispectral imagery is generally acquired in four bands: red, green, blue, and near-infrared (NIR). By combining these bands in different proportions, the user can create natural color images that depict the imaged scene. This advantage is offset by a broader spectral resolution and generally lower spatial resolution. With respect to bathymetry mapping from multispectral imagery, these limitations are exacerbated by the few wavelength bands collected by the sensor. Because the NIR and red wavelengths are rapidly attenuated by water, only the green and blue bands remain to derive depth.

A large pool of research exists describing the manner by which depth can be derived using the green and blue bands of multispectral imagery (e.g. Camacho, 2006; Clark, 2005; Densham, 2005; Hogrefe, 2008; Stumpf et al., 2003). Several limitations exist using only these two bands. Clark (2005) showed that shallow water bathymetry can be difficult to derive accurately over high-albedo substrates. Camacho (2006) showed that depths derived from the green and blue bands are sensitive to substrate type. Both of these limitations are significant when considering the utility of using multispectral imagery for bathymetric mapping for safe ship navigation.

The commercial and civilian multispectral satellites (e.g. Quickbird, IKONOS, Landsat-TM) all suffer from the aforementioned limitations with respect to bathymetric mapping because the sensors are all limited to the same 4 bands (although the exact range

of the bands varies slightly between sensors). The prospective launch of the new Worldview-2 satellite in 2009 may provide a means to overcome the limitations of bathymetric mapping using only the green and blue bands. The Worldview-2 spectral images will add four additional bands to the traditional red, green, blue, and NIR bands on previous multispectral satellites. In particular, a yellow band centered at 605nm may provide a significant improvement for bathymetric mapping.

The research conducted for this thesis investigates the possible increase in fidelity of the Worldview-2 satellite to derive bathymetry in water less than 10m deep. The hypothesis being tested is that the additional yellow spectral band on the Worldview-2 multispectral sensor, coupled with spatial resolution approaching that available with hyperspectral imagery, will enable more accurate depth derivation than that acquired from current multispectral satellites.

II. BACKGROUND

A. RADIATIVE TRANSFER FUNDAMENTALS

1. Electromagnetic Theory

Electromagnetic radiation (EMR) comprises radiation from the very long wave, very high energy gamma and X-rays to the very short wave energy microwaves and everything in between. All types of EMR are waveform energy traveling at the speed of light. Long wave EMR is typically measured by its frequency while short wave EMR is measured by its wavelength. Visible light, found in the shorter wavelengths, is described in micrometers or nanometers.

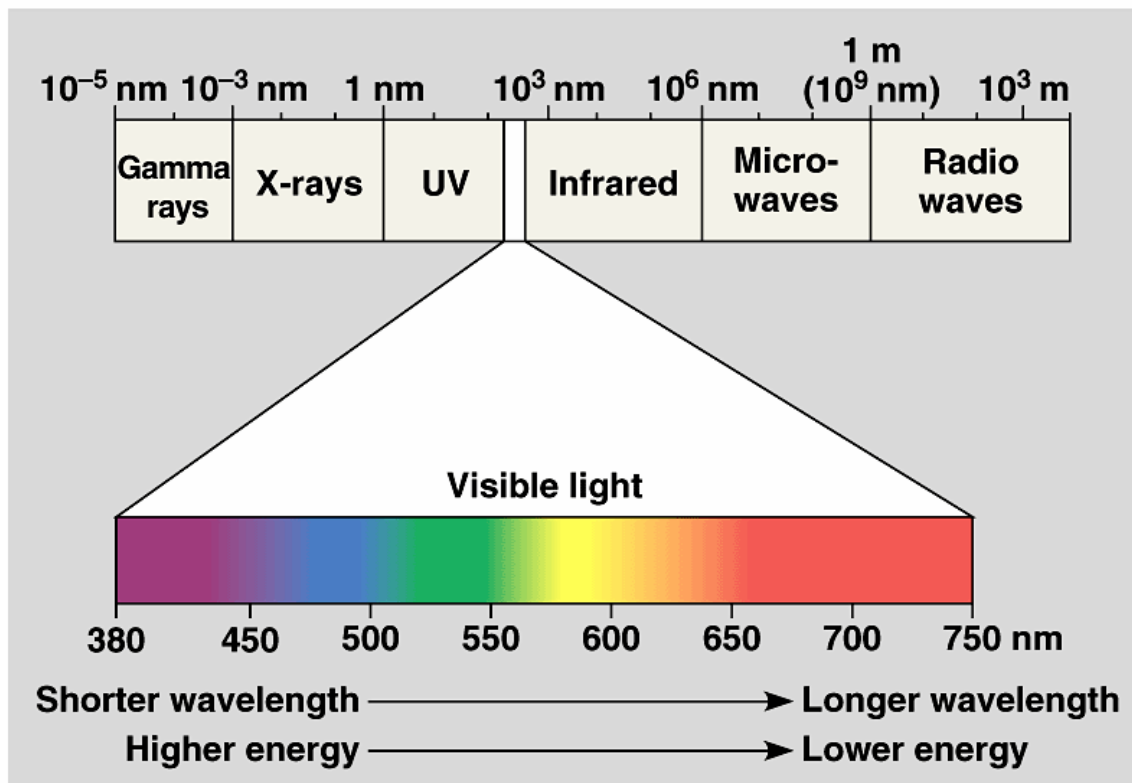


Figure 2. Visible portions of the electromagnetic spectrum (From University of Arkansas at Little Rock 2006).

Remote sensing from optical sensors uses the visible and near-infrared (NIR) frequencies to observe radiation emitted or reflected by the surface. Multispectral sensors typically measure visible radiation in three bands: blue (450-480nm), green (530-560nm), and red (625-675nm). The multispectral sensors also measure radiation in the NIR band at 700-1500nm. Hyperspectral sensors, on the other hand, generally have hundreds of contiguous spectral bands or more, collecting radiation from 400-2500nm.

The light received by a remote sensor undergoes absorption, reflection, scattering and transmittance as it interacts with the surface and atmosphere (Martin, 2004). The specific manner by which it interacts is a function of the frequency, wavelength and angle of incidence of the light (Olsen, 2006). These interactions are quantified by equation (1).

$$L_t(\lambda_i) = L_r(\lambda_i) + L_a(\lambda_i) + T(\lambda_i)L_g(\lambda_i) + t(\lambda_i)L_w(\lambda_i) \quad (1)$$

where $L_t(\lambda_i)$ is the radiance received by the sensor, $L_r(\lambda_i)$ and $L_a(\lambda_i)$ are scattering radiances, T is direct transmittance, $L_g(\lambda_i)$ is the specular reflectance of sunlight from the sea surface, t is the diffuse atmospheric transmittance of the atmosphere, and $L_w(\lambda_i)$ is the water leaving radiance. The final term provides information required for depth retrieval after correcting for the remaining parameters.

B. TEST SITE

Kaneohe Bay, on the eastern side of Oahu in the Hawaiian Islands, was the study site for this research. Kaneohe Bay is sheltered on its seaward side by a large barrier reef. Within the bay itself are numerous patch reefs, fringing reefs and sand patches. Because much of the bay is comprised of coral, the temporal changes in bathymetry should be minimal. Furthermore, the variety of depths and substrates provide a wide range of albedo, and therefore reflectance. Kaneohe Bay, then, is a nearly ideal site for comparison of imagery acquired more than a year apart.

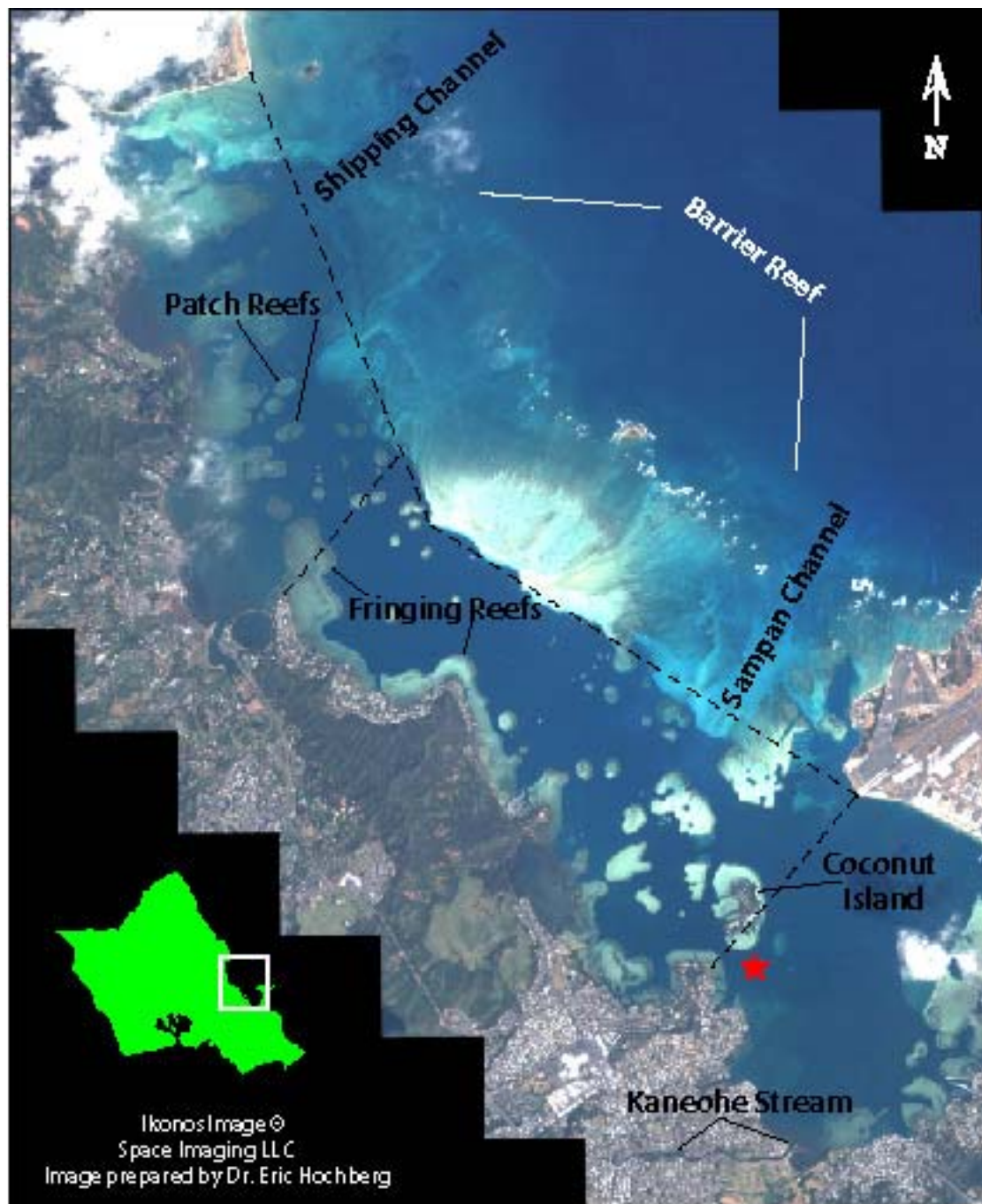


Figure 3. Kaneohe Bay study area

C. MULTISPECTRAL IMAGERY FROM QUICKBIRD

Quickbird is a multispectral and panchromatic imaging satellite owned by DigitalGlobe. It was launched on October 18, 2001 from Vandenberg Air Force Base,

California, and orbits at a 450km, 98 degree sun-synchronous inclination (www.digitalglobe.com). The revisit time is 2-3 days, depending on the latitude to be revisited. Quickbird collects imagery along a 16.5km swath width with a 2.4m resolution at nadir. The spectral bandwidth of the Quickbird multispectral sensor is: blue (450-520nm), green (520-600nm), red (630-690nm) and near-IR (760-900nm).



Figure 4. Quickbird Satellite (from: <http://www.digitalglobe.com/index.php/85/QuickBird>)

D. HYPERSPECTRAL IMAGERY FROM AVIRIS

The AVIRIS (Airborne Visible/Infrared Imaging Spectrometer) is a hyperspectral remote sensor that retrieves upwelling spectral radiance in 224 contiguous bands, encompassing the 400-2,500nm wavelengths. The AVIRIS is flown on four different aircraft types operated by the Jet Propulsion Laboratory. The image used in this research was acquired from the AVIRIS mounted on a Twin Otter turboprop. The AVIRIS operates in a “whisk broom” fashion, sweeping back and forth to collect upwelling radiance along the flight line. The Twin Otter, typically flying at roughly 4km altitude and 130km/hr, collects imagery with a 4m square pixel resolution and 2km swath width (<http://aviris.jpl.nasa.gov/html/aviris.concept.html>). The AVIRIS has a scan rate of 12Hz, a 10nm nominal channel bandwidth, and a 34 degree total field of view (<http://aviris.jpl.nasa.gov/html/aviris.concept.html>).

As the data is collected, it is recorded on the instrument along with aircraft location and orientation. A typical “scene” would consist of a 10km x 2km area collected over consecutive swaths. After retrieval, the data is processed and stored for dissemination to interested users.

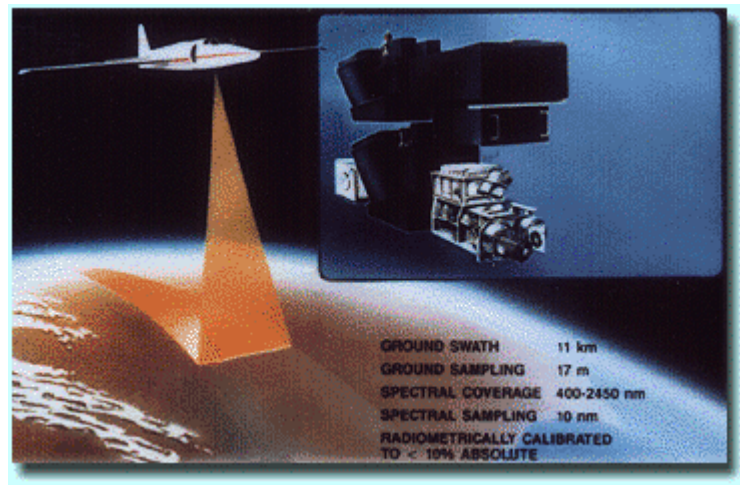


Figure 5. AVIRIS instrument mounted on an ER-2 aircraft. (From: <http://aviris.jpl.nasa.gov/html/aviris.overview.html>)

E. MULTISPECTRAL IMAGERY FROM WORLDVIEW-2

Worldview-2 is a multispectral satellite scheduled for launch from Vandenberg Air Force Base, California in 2009. The satellite will occupy a 770km high sun synchronous orbit with a 100 minute period. Like Quickbird, Worldview-2 has a 16.4km swath width, a 1.1-3.7 day revisit time, and the spectral sensor will have similar spectral bandwidth of blue, green, red, and near-IR. However, Worldview-2 has a spatial resolution of 1.84m and several additional spectral bands: an additional blue band centered at 425nm, a yellow band centered at 605nm, a red edge band centered at 725nm and a long wavelength near-IR band centered at 950nm. The satellite will also have a panchromatic sensor with about 0.5m spatial resolution (http://www.digitalglobe.com/downloads/WV1_WV2_SpectralResponse.pdf).

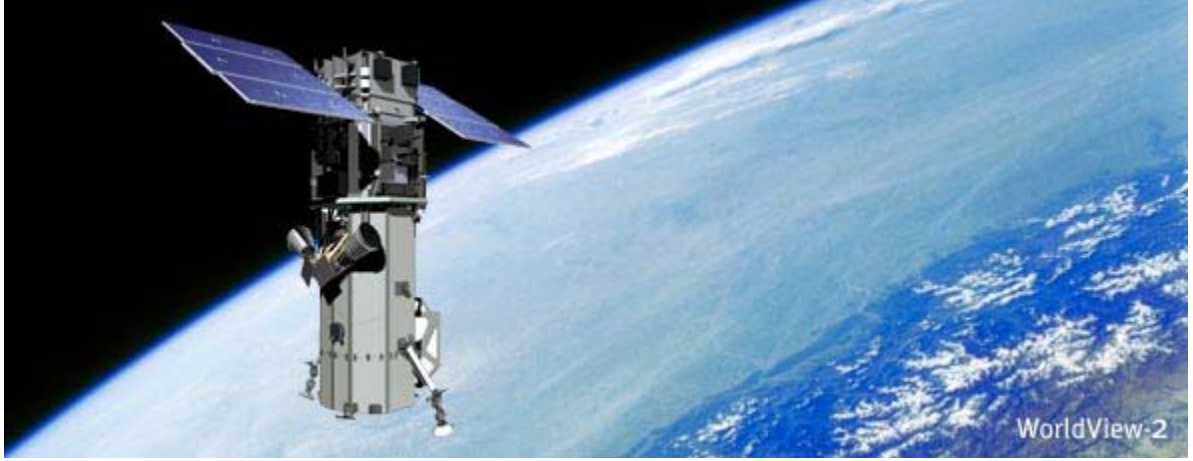


Figure 6. Worldview-2 Satellite. (From <http://www.digitalglobe.com/index.php/88/WorldView-2>)

F. BATHYMETRY DERIVATION FROM REMOTELY SENSED DATA

There are several methods available to derive bathymetry from remotely sensed images, generally segregated into “linear methods” and the “ratio methods”. Both methods are based upon the principle that light is attenuated through interaction with the water column, and the depth to which light penetrates water is dependent upon the light’s wavelength. This relationship is given by the equation:

$$I_d = I_0 \cdot e^{-pk} \quad (2)$$

where I_d is the intensity of light, I_0 is the intensity of incident light, p is the length of the path of water through which the light passes, and k is the attenuation coefficient that varies with wavelength. The shortest wavelengths penetrate the deepest while the longest wavelengths penetrate the shallowest, if at all.

Depth and bottom reflectance affect radiance through the equation:

$$R_{rs} = (A_b - R_\infty)e^{(-gz)} + R_\infty \quad (3)$$

where A_b is the irradiance reflectance of the bottom (albedo), R_∞ is the reflectance of the water column, g is a function of the diffuse attenuation coefficient for upwelling and downwelling light, and z is depth (Lyzena, 1978). This equation is solved for depth by:

$$z = g^{-1}[\ln(A_d - R_\infty) - \ln(R_{rs} - R_\infty)] \quad I_d = I_0 \cdot e^{-pk} \quad (4)$$

where I_d is the intensity of light.

The linear methods (Benny and Dawson, 1983; Jupp, 1988; Lyzenga, 1978) make two primary assumptions. The first assumption, common to both methods, is that light will penetrate water to a degree dependent upon its wavelength (Green et al., 2000). The second assumption is that water quality is homogeneous throughout the image (Green et al., 2000). Additional assumptions exist depending on the method used. For example, Benny and Dawson (1983) assume that the substrate albedo is homogeneous. This presents significant limitations in an environment such as Kaneohe Bay, Hawaii.

Stumpf et al., (2003) proposed a “ratio method” that, to some extent, overcomes the limitations of varying substrate albedo. The method builds upon the principle of light attenuating exponentially with depth, but proposes that by using two bands to derive depth, the effects of substrate albedo are minimized (Stumpf et al., 2003). This principle is explained mathematically as follows.

Equation (2) describes the attenuation of light with depth by Beer’s Law. Lyzenga (1978) described the relationship of observed reflectance with depth and bottom albedo. Lyzenga’s (1978) equation quantifies depth as a function of reflectance and albedo by equation (5).

$$z = g^{-1}[\ln(A_d - R_\infty) - \ln(R_w - R_\infty)] \quad (5)$$

where z is depth, g is a function of the diffuse attenuation coefficients for both downwelling and upwelling light, A_d is the bottom albedo, R_∞ is the water column reflectance if the water were optically deep, and R_w is observed reflectance.

The depth calculated in this manner is, as previously stated, dependent upon albedo. Therefore, while the albedo of the two substrates at the same depth would be considerably different, the albedo of the two substrates at very different depths may look very similar. By equation (3), the depth would be incorrectly calculated for one of these two substrates.

The ratio method addresses this limitation by comparing the attenuation of two bands against one another rather than using albedo as a variable in depth calculation. Different bands attenuate at different rates, therefore, one band will be less than the other. The ratio between the two bands will change with depth. The change in bottom albedo should affect both bands similarly, but the change in attenuation with depth will be greater than the change attributable to bottom albedo so that the ratio between the two bands should remain similar over different substrates at the same depth (Stumpf et al., 2003).

The ratio method is described mathematically by equation (6):

$$Z = m_1 \frac{\ln(nR_w(\lambda_i))}{\ln(nR_w(\lambda_j))} - m_0 \quad (6)$$

where Z is depth, m_1 is a tunable constant to scale the ratio to depth, n is a constant to ensure the ratio remains positive under all values, R_w is observed reflectance, and m_0 is the offset for a depth of 0m.

III. METHODS

A. METHODOLOGY OVERVIEW

The purpose of this research is to evaluate the value added by the yellow band on the Worldview-2 satellite to derive bathymetry from multispectral imagery. Because the Worldview-2 satellite will not be operational until after publication of this research, it is necessary to use an existing sensor as a “proxy sensor” to perform the experiments. No commercial multispectral sensor is available with a yellow band, therefore a hyperspectral sensor is used instead.

As mentioned previously, hyperspectral imagery has narrower bandwidth, higher resolution, and more than 200 additional bands from which to choose. Before using a hyperspectral sensor to simulate a multispectral sensor, it is desirable to demonstrate the equivalency between a multispectral and hyperspectral sensor for bathymetric derivation. This is accomplished in this research by comparing a “control” image acquired by the multispectral sensor on the Quickbird satellite to a hyperspectral image acquired by the AVIRIS sensor.

These two sensors were chosen for several reasons. First, in order to compare the imagery between the two sensors, it was necessary to have imagery that was acquired by both sensors over the same area. Second, because Quickbird has the highest resolution of the available commercial multispectral satellites, it is the closest to the resolution of the Worldview-2 satellite and, therefore, the best available satellite for comparison. Finally, AVIRIS imagery resolution varies tremendously depending on which aircraft carries the instrument. The ER-2 collects imagery with a pixel resolution of 20m diameter, a resolution unusable for this type of research. Therefore, Twin Otter-collected imagery was highly desirable.

The general processing techniques for the two images are very similar; the specifics are detailed in the following sections. In general, the steps used to derive bathymetry from the two images are:

1. Calibrate the imagery to absolute radiance.
2. Apply masks.
3. Convert image to reflectance.
4. Classify and spatially subset image.
5. Determine relative bathymetry.
6. Determine absolute bathymetry.

Each step is applied to both the Quickbird and AVIRIS images. The bathymetry is derived from the Quickbird image by applying the ratio method using the green/blue bands. The same method is used to derive bathymetry from the AVIRIS image. By demonstrating that both images exhibit the same errors and limitations in depth derivation, it is possible to use the yellow band from the AVIRIS sensor to perform additional depth derivations with the implication that the results are applicable to multispectral imagery as well.

As described previously, the AVIRIS sensor collects 224 contiguous bands, compared to the four bands collected by Quickbird. Therefore, four bands were chosen from the AVIRIS sensor to be representative of a multispectral sensor, based upon the center effective wavelength (CEW) of the four multispectral bands. Table 1 depicts the AVIRIS bands chosen next to the corresponding multispectral bands.

Color	AVIRIS Band	Multispectral CEW
Blue	Band 13 (481.6237 nm)	482 nm
Green	Band 19 (539.4518 nm)	536 nm
Yellow	Band 26 (606.9716 nm)	605 nm
Red	Band 31 (655.2352 nm)	652 nm
NIR	Band 50 (815.9965 nm)	816 nm

Table 1. AVIRIS bands used for image processing

The processing for both images was conducted using a software package called ENVI 4.5 (Environment for Visualizing Images). ENVI provides numerous utilities for the visualization, analysis and presentation of digital imagery. It has the capability to process both multispectral and hyperspectral imagery, and the available tools allowed the various equations delineated in this research to be applied directly to the images.

B. QUICKBIRD

The multispectral image used in this research was collected from the Quickbird satellite on March 13, 2003. The image was acquired from Digital Globe via the National Geospatial-Intelligence Agency (NGA).

1. Calibration

Quickbird imagery is distributed in units of relative radiance, recorded as digital numbers (DN) by the sensor (Green et al., 2000). Digital Globe provides calibration information in a metadata file that is used to convert the pixels in the imagery from DN to absolute radiance. The calibration routine is expressed mathematically as:

$$L_{Pixel,Band} = absCalFactor_{Band} * q_{Pixel,Band} \quad (7)$$

where $L_{Pixel,Band}$ is the absolute radiance for each pixel, for each band; $absCalFactor_{Band}$ is provided by Digital Globe in the metadata file, and $q_{Pixel,Band}$ is the original DN value of the pixel per band. ENVI provides a preprocessing utility that calculates this calibration automatically. The ENVI utility was used to calibrate the Quickbird image used for this research. The resultant image is in units of $(\mu W)/(cm^2 * nm * sr)$.

2. Spatial Subsetting

The second pre-processing step is to remove land areas and other areas not required for the bathymetry calculation. A mask was manually created in ENVI to remove areas outside of the study region.

3. Conversion to Top-of-Atmosphere Reflectance

In order to compare images acquired by different sensors, it is necessary to convert the images to reflectance (Green et al., 2000). The radiance of an image depends

on how the image is illuminated (irradiance), which is a factor of time of day, season, latitude at which the region lies, etc. Reflectance is a ratio of radiance to irradiance, therefore it creates a standard by which images acquired at different times by different sensors can be compared.

The ENVI bandmath utility was used to convert the Quickbird image to reflectance. The Quickbird image metadata file contains the Earth-sun distance, solar zenith angle, and image acquisition date. Equation (8) shows how the information allows reflectance to be calculated:

$$\rho_{\lambda_{Pixel}, Band} = \frac{L_{\lambda_{Pixel}, Band} * d_{ES}^2 * \pi}{E_{sun_{\lambda_{Band}}} * \cos(\theta_s)} \quad (8)$$

The bandmath expression is calculated for each band individually. Afterwards, all bands are compiled into a single image with a reflectance value for each pixel.

4. Supervised Classification

Camacho (2006) determined that the ratio method using the green and blue bands is sensitive to substrate type. In order to minimize the error introduced by heterogeneous substrates in this research, a supervised classification was performed on the image. No ground truth information was available for the image; therefore, a minimum number of classifications was desirable.

Regions of Interest (ROI) were established on the Quickbird image corresponding with sand, optically deep water, and reef/non-sand substrate. Multiple ROIs were created for each type where the different substrates were clearly discernable.

The ROIs were then used as training sites for a supervised classification of the Quickbird image. The desired number of classes was set at three (sand, deep water, reef/non-sand substrate). The maximum likelihood classification routine was run in ENVI. The results were spatially segmented into separate images for bathymetric derivation. Figure 7 shows the completed classified image (left) compared to the Quickbird top-of-the-atmosphere reflectance image (right). Brown color represents non-sand substrate, green is sand substrate, and blue is optically deep water. The majority of

the area encompassing sand-classified substrate was not collected by the AVIRIS image, so the non-sand substrate (brown in the classified image) was used for all subsequent depth derivation.

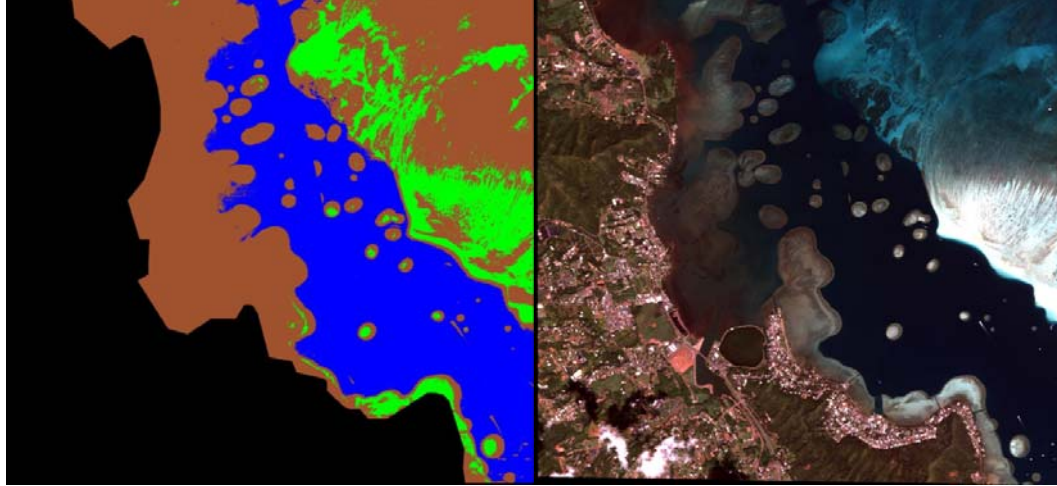


Figure 7. Supervised classified Quickbird image (left). Green is sand, brown is non-sand substrate, and blue is optically deep water. Quickbird reflectance image (right).

5. Bathymetric Derivation

The first step to derive bathymetry from the image is to determine relative bathymetry using the natural log transform of the reflectance values. Equation (9) shows the ratio expression used for relative bathymetry:

$$\frac{\ln(1000 * b_1)}{\ln(1000 * b_2)} \quad (9)$$

where b_1 is the blue band reflectance value, and b_2 is the green band reflectance value. The reflectance values are multiplied by 1000 (the n value in equation (6)) to ensure that the logarithms remain positive for all reflectance values.

The next step is to calibrate the relative bathymetry to absolute bathymetry. A series of points from a digital nautical chart near easily identifiable features were extracted into a spreadsheet as ground truth data. These points were then regressed against the relative bathymetry values using equation (6) to derive absolute bathymetry for the entire image. The Quickbird regression is provided in Appendix B.

After conversion to absolute bathymetry, a -0.8 ft. correction was applied to correct for tides. Figure 8 depicts the tides at the time of image collection (10:59 AM HST, GMT-10).

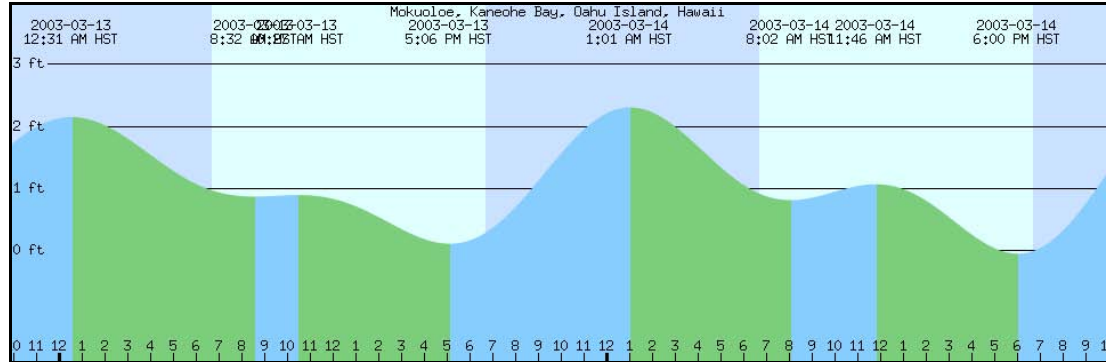


Figure 8. Kaneohe Bay tides for 10:59 AM, HST (GMT-10)

C. AVIRIS

The AVIRIS image used in this research was collected by a Twin Otter aircraft on March 1, 2005. The collect time start was 2055 GMT; the end time was 2059 GMT. The aircraft altitude during collection was 12,500 ft. and the ground speed was 78 knots. The image was acquired from the Jet Propulsion Laboratory by the author.

1. Calibration and Spatial Subsetting

Unlike the Quickbird image, AVIRIS imagery is calibrated to absolute radiance before it is provided to the user. Therefore, no calibration was performed on the AVIRIS image in this research. A mask was manually applied to the image to remove land features.

2. Conversion to Top-of-Atmosphere Reflectance

As mentioned previously, it is necessary to convert imagery to reflectance to compare images collected by different sensors. Several techniques exist to convert hyperspectral imagery to reflectance. ENVI provides a utility called “Internal Average Relative Reflectance” that evaluates the average reflectance from the image and uses the

average value to remove atmospheric effects. This technique is useful when no ground truth atmospheric data is available (ENVI Help file). Because no ground truth data regarding the irradiance and atmospheric effects were available, this technique was chosen over other, more robust techniques (e.g., Goodman et al., 2008; Mustard et al., 2001).

3. Regions of Interest

Regions of interest were created in the same areas that were used in the Quickbird image.

4. Supervised Classification

A supervised classification was performed on the AVIRIS image using the same settings as those used for the Quickbird image; three classifications were provided for sand, reef/non-sand substrate, and optically deep water. The resulting classified image very closely matched the Quickbird classified image. All depth derivation was conducted on the reef/non-sand substrate subsetting image. Figure 9 shows the AVIRIS reflectance image (left) next to the AVIRIS classified image (right). Figure 10 shows the Quickbird classified image (left) compared to the AVIRIS classified image (right).

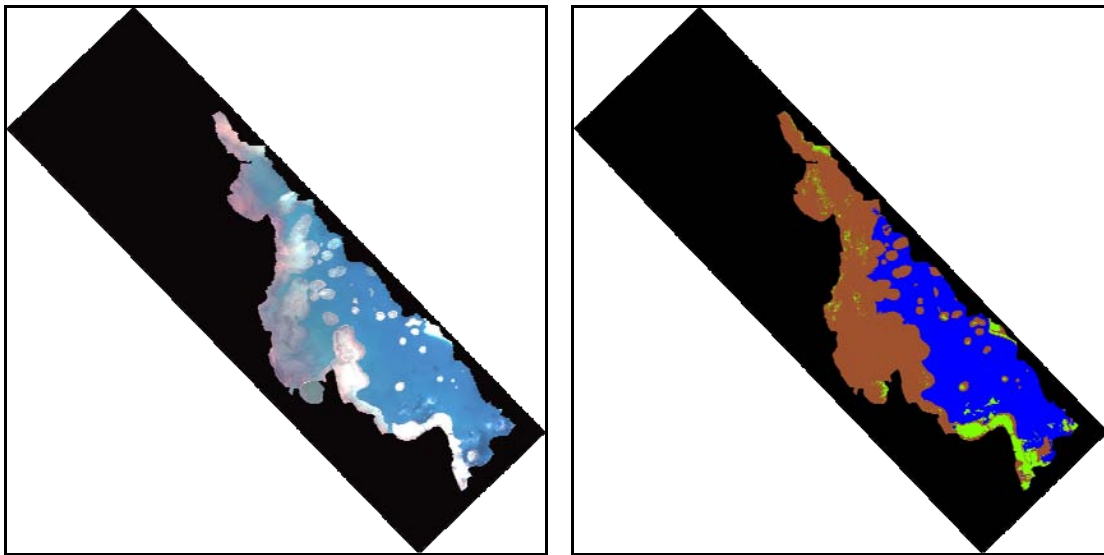


Figure 9. AVIRIS classified image (left) and AVIRIS reflectance image (right). On the classified image, green is sand, blue is optically deep water, brown is reef.

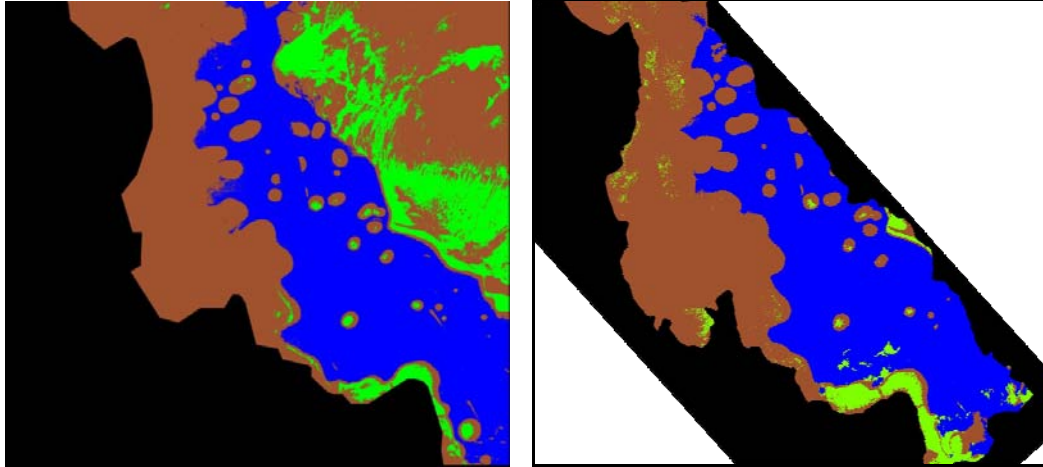


Figure 10. Quickbird classified image (left) and AVIRIS classified image (right). The brown reef-classified areas match well between the two images.

5. Bathymetric Derivation

Bathymetry was derived on the AVIRIS imagery using the same techniques as the Quickbird imagery. Relative bathymetry was derived first. Then the relative bathymetry values were regressed against ground truth points to derive absolute bathymetry. The AVIRIS regressions are provided in Appendix A. Finally, a -0.4 ft. tide correction was applied to the final imagery (Figure 11).

a. Green/blue Ratio

The first bathymetric map was calculated using multiple regressions of the green and blue bands as described for the Quickbird imagery.

b. Yellow/green Ratio

The second bathymetric map was calculated using multiple regressions of the yellow and green bands as described for the Quickbird imagery. Equation (6) provides the ratio where b_1 is the green band and b_2 is the yellow band.

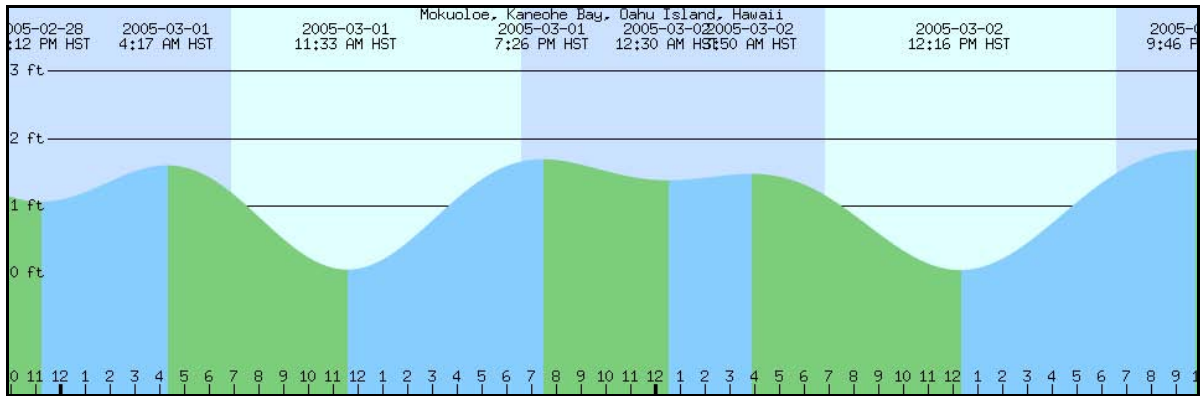


Figure 11. Kaneohe Bay tides for March 1, 2005 at 12:55 PM HST (GMT-10)

c. Yellow/blue Ratio

Finally, a bathymetric map was calculated using multiple regressions of the yellow and blue bands using the same techniques used previously. Equation (6) provides the ratio where b_1 is the blue band and b_2 is the yellow band.

THIS PAGE INTENTIONALLY LEFT BLANK

IV. RESULTS

A. BATHYMETRY USING THE GREEN/BLUE RATIO

Figure 12 shows the results from the AVIRIS reef classified image using the green/blue ratio (left) compared to the Quickbird reef classified image using the green/blue ratio (right). Figure 13 shows the digital nautical chart used for ground truth depths (left) and the AVIRIS reflectance image showing the heterogeneous albedo (right). Both images in Figure 12 show similar depth classifications and regions of significant error in the derived depth.

The area in the vicinity of the box labeled ‘A’ (Figure 12) shows a shallow reef area with a reef crest on the right side. The reef area as shown on the digital nautical chart depicts shallow depths of 1-2 feet. On both the AVIRIS and Quickbird images, the depths are negative (emergent) in the immediate location of the box. The reef area to the left has depths from 1-2 feet on the digital nautical chart (Figure 14), and 1-20 feet on both the AVIRIS and Quickbird images. The reef crest to the right of the box has a depth of 1 foot on the digital nautical chart, and depths of 18-21 feet on both images.

The area in the vicinity of the box labeled ‘B’ (Figure 12) shows a reef area sloping from southwest to northeast, with a shallow depth of 1 foot at the southwestern most point to a maximum depth of about 25 feet to the northeast before the image is masked by the optically deep water classification. Both the AVIRIS image and the Quickbird image show a deep area immediately in the vicinity of the box with shallower areas from 1-5 feet on the northerly and southerly sides. However, the digital nautical chart shows a sloping bathymetry that does not have a deep region surrounded by two shallower regions. Both images appear to be confused by the multi-colored reef clearly shown in the AVIRIS reflectance image (Figure 13). The Quickbird image in particular shows bathymetry strongly corresponding to varying substrate albedo.

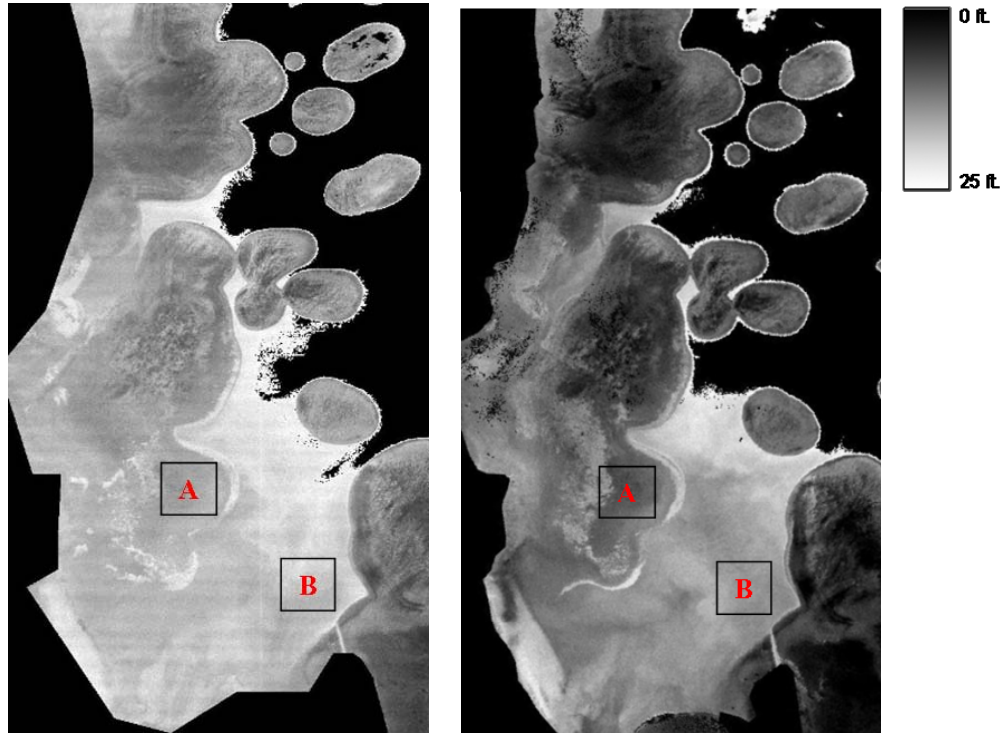


Figure 12. Quickbird Reef Classified Bathymetry from green/blue ratio (left); AVIRIS Reef Classified Bathymetry from green/blue ratio (right). Light colors represent deeper depths, darker colors represent shallower depths. The black regions are masked out.

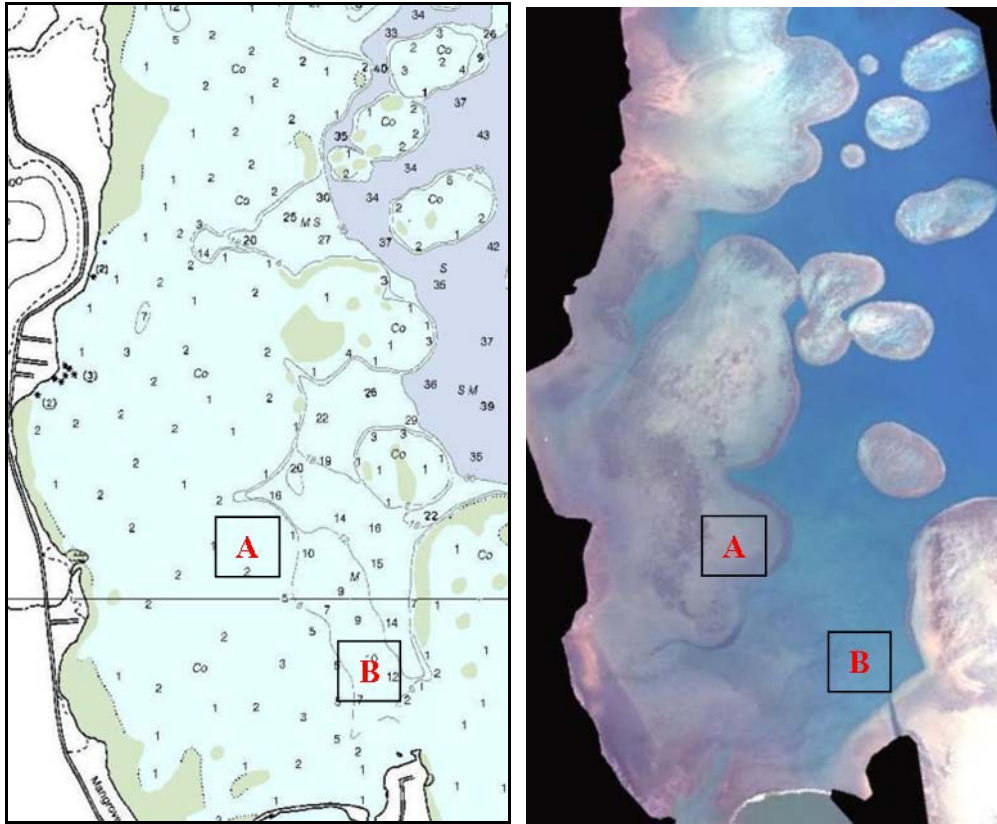


Figure 13. Digital nautical chart (left) showing ground truth bathymetry with AVIRIS reflectance image (right).

B. BATHYMETRY USING THE YELLOW/GREEN RATIO

Figure 14 shows the AVIRIS reef classified bathymetry using the yellow/green ratio. In this image, the derived bathymetry very closely matches the actual bathymetry. The reef area in the immediate vicinity of box 'A' shows depths of 1-3 feet. The reef area to the west of box 'A' has depths from 0-2 feet. The reef crest to the east of box 'A' shows depths from -1 (emergent) to 2 feet.

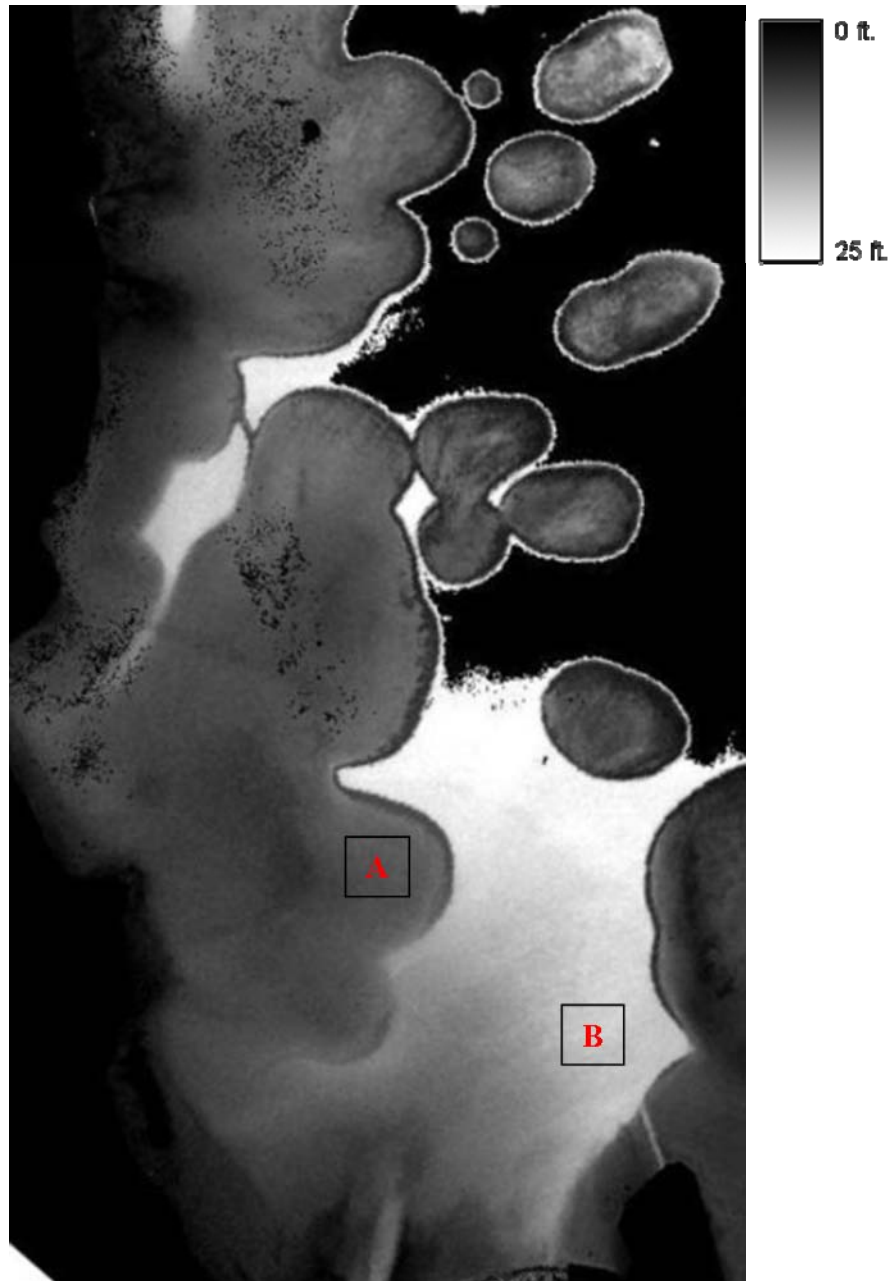


Figure 14. AVIRIS Bathymetry from yellow/green ratio. Dark regions represent shallow bathymetry, lighter regions represent deep bathymetry.

The derived depths in the vicinity of box 'B' are also very close to the actual bathymetry. The emergent reef near the small channel southwest of box 'B' and the

small emergent features just outside of the channel (bottom-center of Figure 12) show well. The derived depths show a very smooth slope from southwest to northeast independent of the bottom albedo.

C. BATHYMETRY USING THE YELLOW/BLUE RATIO

Figure 15 shows the derived bathymetry using the yellow/blue ratio on the AVIRIS reef classified image. In the immediate vicinity of box 'A' the depths agree well with the actual bathymetry, ranging from slightly emergent to 2 feet depth. To the west of box 'A' the depths also agree well with the actual bathymetry - depths ranging from 1-2 feet. The reef crest on the east side of box 'A' is well-resolved with shallow depths ranging to 5-6 feet at the crest, dropping to 10-13 feet as depicted in the digital nautical chart.

The region near box 'B' is also well resolved. The derived depths slope evenly between the channel to the southwest and the drop-off to the northeast. The derived bathymetry shows slightly more variability, but whether this is due to albedo or actual variability in the bathymetry is difficult to discern because the derived depth variation agrees very closely with the actual digital nautical chart. The maximum resolvable depth appears to be about 21 feet, as the depths northeast of box 'B' do not derive deeper than that. Ground truth points were provided in the regression to a maximum of 25 feet.

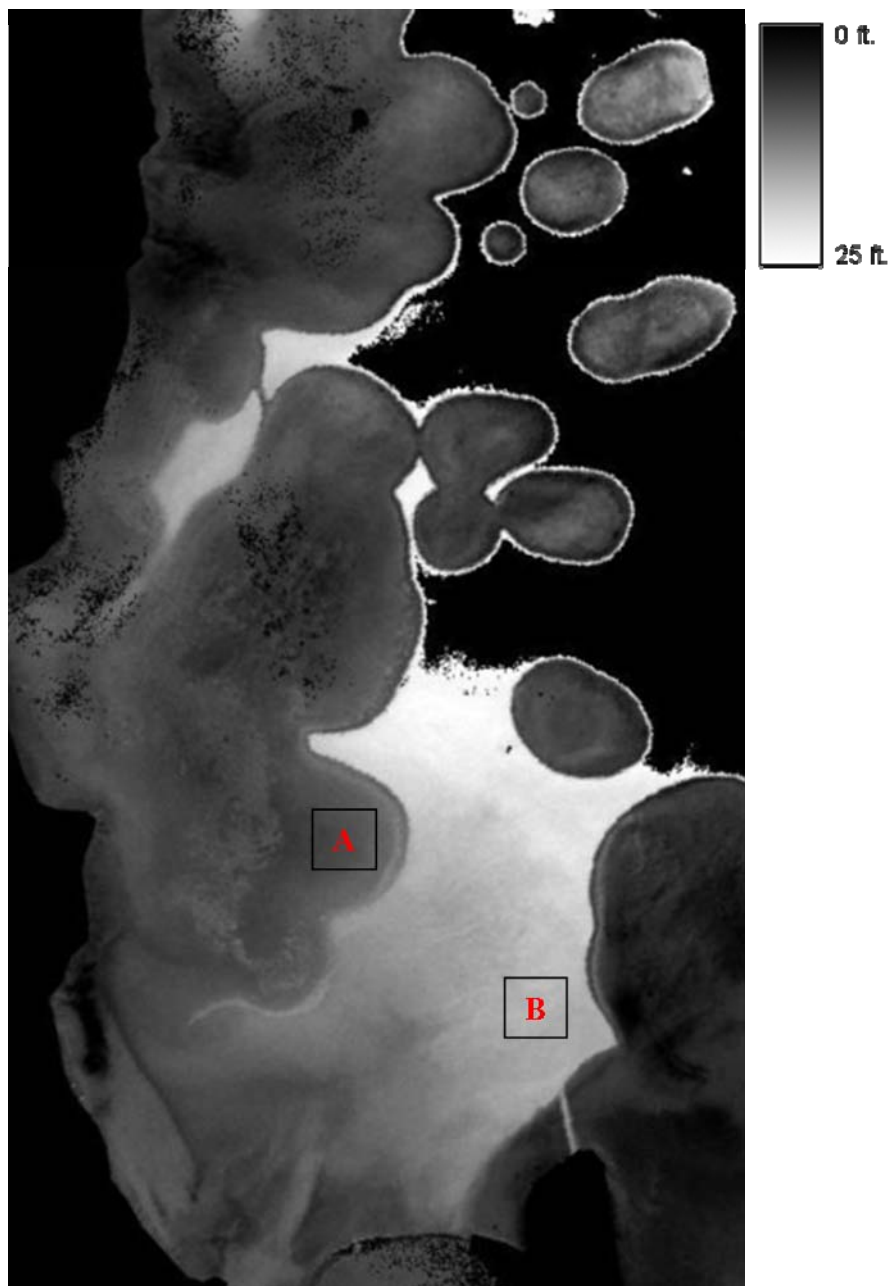


Figure 15. AVIRIS reef classified bathymetry using the yellow/blue ratio.

D. TRANSECTS

In order to quantify the differences between the three ratios tested, two transects were created using the ROI polyline tool in ENVI. The ROI was exported to each image. The ROI was also manually placed on the digital nautical chart. Ground truth depths were extracted from the digital nautical chart where published soundings intersected or nearly intersected the transect line.

The ROI was exported to an excel spreadsheet. Extracted ground-truth depths were manually input into the spreadsheet as well. The transects and ground-truth depths are depicted in Figures 17 and 20.

One of the major limitations to using a nautical chart for ground truth depth is the poor resolution of soundings compared to more robust methods. Only a small fraction of the soundings taken during a survey are displayed on a chart (Bowditch, 1995). Additionally, even a thorough survey may not discover every rock, pinnacle or coral head (Bowditch, 1995). This presents significant difficulty when trying to utilize bathymetry along a transect with only a few soundings used as ground truth depths.

Very late in this research a SHOALS survey for Kaneohe Bay in the region of the study was acquired. While the survey was acquired too late to use for the ground truth bathymetry, it could be used to determine relative error for the nautical chart ground truth depths. Figure 16 shows a section of the SHOALS survey. The depth values from adjacent soundings vary about 0.5-1.0m (1 ½ - 2 ft.). Therefore, the ground truth depths used for transects 1 and 2 show +/- 2 ft. error bars to account for the variability caused by the reef substrate.

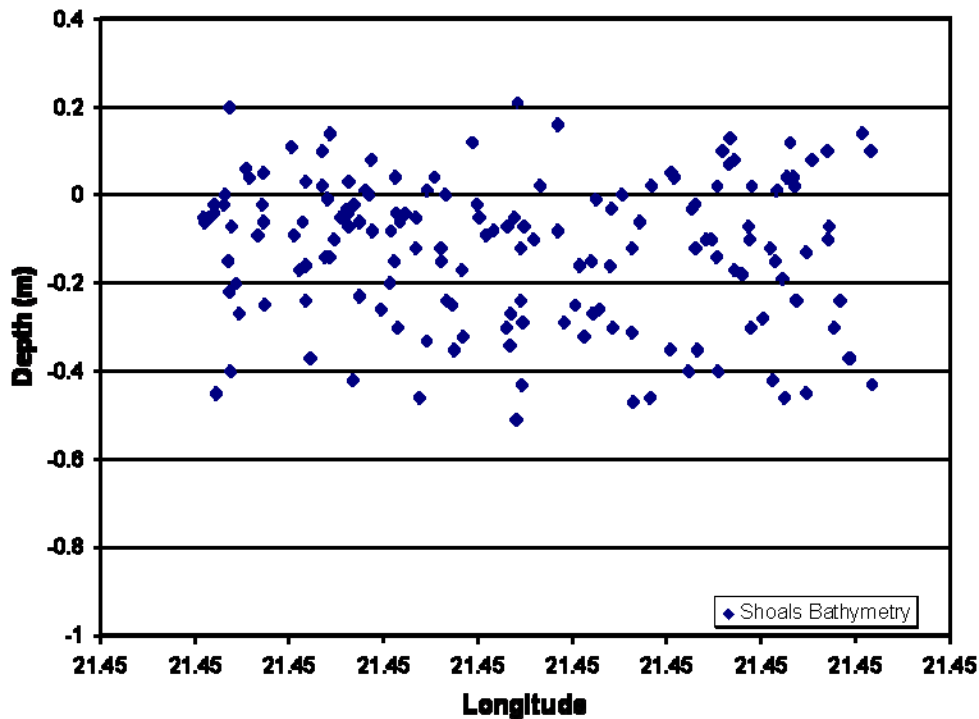


Figure 16. SHOALS bathymetry showing depth variability of the reef along a short portion of a survey line in the study area. Retrieved from the Hawaii Coastal Geology Group online at:
(<http://www.soest.hawaii.edu/coasts/data/oahu/shoals.html>)

1. Transect 1

Transect 1 runs from the reef flat on the west side of the image to the emergent reef crest on the eastern side of the image (Figure 17). The transect captures the erroneous depths in the green/blue ratio of the reef flat and first reef crest as well as the deep channel between the two reef sections.

Figure 18 shows the depths plotted along the Transect 1. Starting on the reef flat on the west side of the image, the ground truth depths range from 0-2 feet, but the reef is not emergent. The green/blue ratio shows significant error in the derived depth in the shallow water. Pixels 0-10 capture the dark reef substrate in the center of the reef flat. The green/blue ratio interprets this substrate as deep water from 5-13 feet depth. From pixels 10-40 the green/blue ratio interprets the lighter area as emergent. Pixels 65-70

The yellow/green ratio interprets the shallow water from pixels 1-60 very well. Additionally, the yellow/green ratio captures the depth over the reef crest very accurately and independent of albedo. As the depth increases beyond the reef crest, the yellow/green ratio overestimates the depth at about 18 feet compared to the ground truth depths of 12-15 feet.

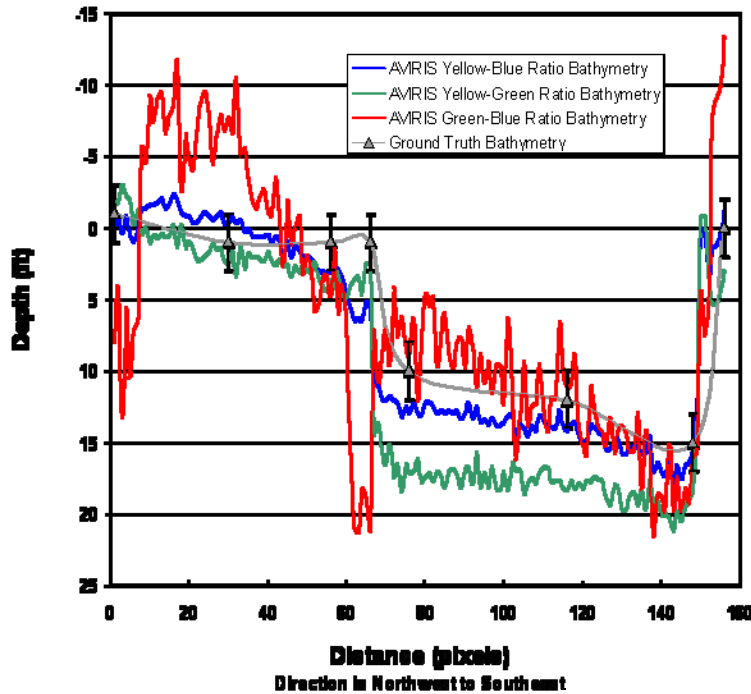


Figure 18. Transect 1 bathymetry. The error bars represent uncertainty in actual ground truth depth as depicted in Figure 16. Negative values are emergent.

A Pearson correlation statistic was evaluated for each ratio to determine the correlation between the derived depths and the ground truth depths ($n = 6, df = 4$). The results, depicted in Figure 19, show that the depths are poorly correlated for the green/blue ratio ($r = 0.529$). The depths are very well correlated for the yellow/green ratio ($r = 0.979, p > .99$) and the yellow/blue ratio ($r = 0.945, p > .99$) with a greater than 99% confidence for both ratios.

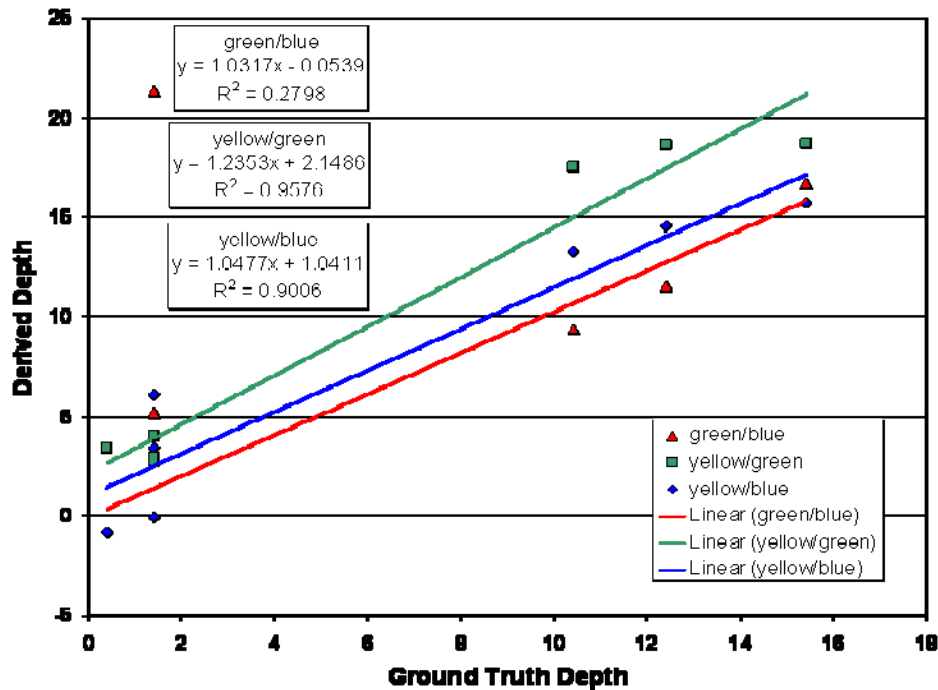


Figure 19. Transect 1 derived depth and ground truth depth correlations for each ratio tested.

2. Transect 2

Transect 2 runs from the deep channel between the east reef crest and a patch reef, southwest to the shallow and emergent reef near land (Figure 20). The transect captures the gradually sloping reef substrate with a depth range from emergent to about 25-30 feet.

The transect begins very close to the 30 feet bathymetry line on the digital nautical chart. The exact depth at the beginning of the transect is difficult to discern with 100% accuracy from the nautical chart, however. The green/blue ratio captures the deepest depth accurately from pixels 0-20. The green/blue ratio also captures the depths well between pixels 20-170, but the depths show substantial variability of as much as 10 feet between adjacent pixels. From pixels 170-300 the green/blue ratio shows as much as 20 feet of variability in derived depth, corresponding to changing substrate albedo in this

region. Beyond pixel 360 the green/blue ratio interprets the depths as emergent while the digital nautical chart shows shallow depths of about 1-2 feet.

The yellow/blue ratio is difficult to interpret between pixels 0-60. The derived depths appear to be underestimated until pixel 60, near the 22 foot sounding on the digital nautical chart. The 16 foot sounding is captured well and the remaining portion of the transect is in agreement with the ground truth soundings.

The yellow/green ratio underestimates the depth initially, but agrees with the green/blue ratio from pixels 20-60. From pixels 60-180 the yellow/green ratio overestimates the depth, varying from the ground-truth depth by about 3-5 feet. From pixel 180-270 the yellow/green ratio agrees well with the yellow/blue ratio and the ground truth depths. At pixels 270-290 the yellow/green ratio shows an emergent spike in depth. This could represent an actual patch of emergent reef or it could be erroneous, as the depth is between emergent and 2 feet on the digital nautical chart. Beyond pixel 290 the yellow/green ratio derived depths agree well with the ground truth depth.

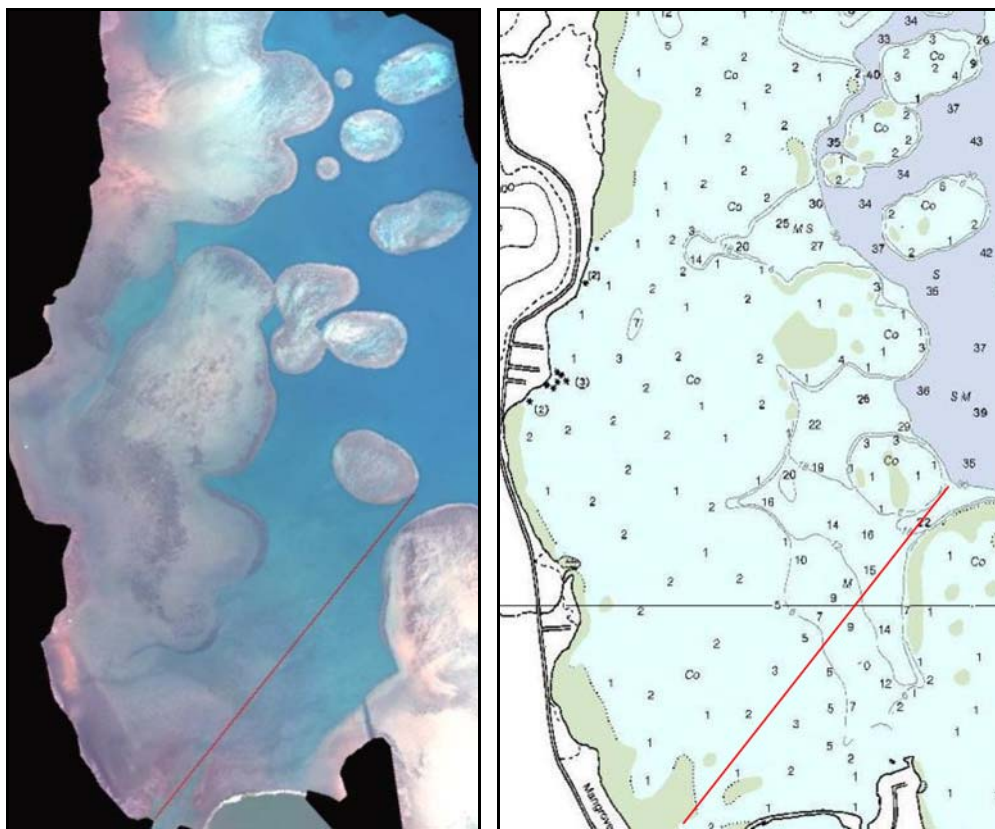


Figure 20. Transect Line 2. The AVIRIS reflectance image is on the left, the digital nautical chart used for ground truth is on the right. The transect runs from the northeast (pixel 1) to southeast (pixel 378).

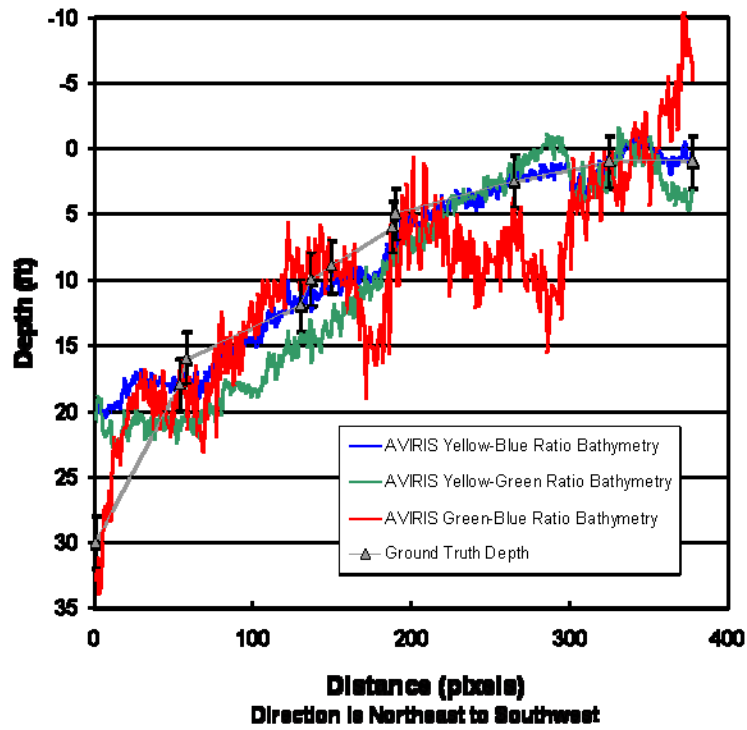


Figure 21. Transect 2 bathymetry. The error bars represent uncertainty in actual ground truth depth as depicted in Figure 16. Negative values are emergent.

A Pearson correlation statistic was evaluated for transect 2 as well to determine the correlation between the derived and ground truth depths for each ratio ($n=10, df=8$). The results show that all three ratios exhibit strong correlation with greater than 99% confidence; green/blue ($r=0.99, p>.99$), yellow/green ($r=0.887, p>.99$), yellow/blue ($r=0.945, p>.99$). The results are depicted in Figure 22.

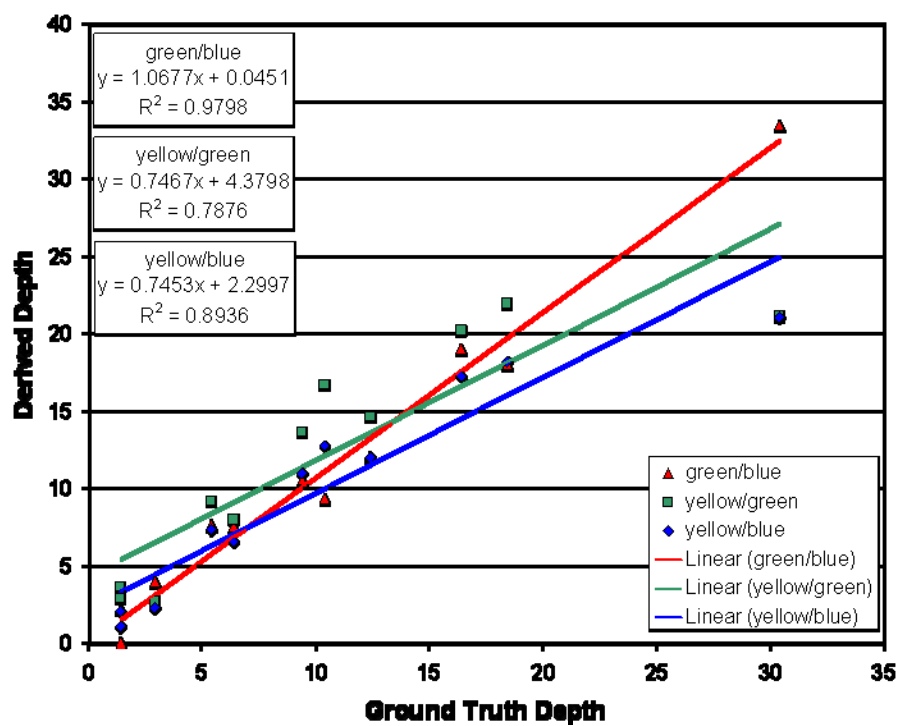


Figure 22. Transect 2 derived depth and ground truth depth correlations for each ratio tested.

THIS PAGE INTENTIONALLY LEFT BLANK

V. DISCUSSION

This study demonstrates the utility of using the yellow band in addition to the typical green and blue bands to derive bathymetry using the ratio method. Stumpf et al. (2003) hypothesized that the ratio algorithm could be used to derive bathymetry independent of substrate albedo. Camacho (2006) demonstrated that the ratio method could be improved upon by tuning the ratio parameters (m_0 and m_1) specifically to different substrates. However, both studies confirmed the limitation of the ratio algorithm for deriving depth values in shallow water with high reflectance. This study overcomes this limitation by using the yellow band in the ratio algorithm.

The sensitivity of the green/blue ratio to shallow water reflectance is clearly shown over the reef flat and reef crest area in Figure 12. The algorithm appears to misinterpret the low albedo reef substrate as deep substrate due to its low reflectance. The reef flat area in particular shows the sensitivity of the algorithm using the green/blue ratio over shallow water with higher reflectivity where the depth is derived as emergent.

Comparing the green/blue ratio-derived depth values to those derived with the yellow/blue ratio, the error seems to be induced by the blue band. The reef flat area in Figure 17 is very shallow with ground truth depths of 0-2 feet from pixels 0-60. The green/blue ratio derives this region as deep in the dark albedo area and emergent over the lighter albedo area. The yellow/blue ratio also shows some emergent areas from pixels 0-35 and has difficulty deriving accurate bathymetry until the depths drop off after the reef crest near pixel 70.

The reason the ratios utilizing the blue band derive shallow bathymetry poorly is probably linked to the slow attenuation of blue light with depth. Beer's Law, depicted in equation (2), shows that light attenuates exponentially with depth dependent on wavelength. Figure 23 graphically shows the slow attenuation with depth of blue light compared to shorter wavelengths. Camacho (2006) attributed the poor resolution of depth with the green/blue ratio in shallow water to the high apparent reflectance values of the green band. However, the data in this study support the hypothesis that the blue band

shows high apparent reflectance with little attenuation and, in fact, this is what causes the erroneous emergent values with the blue-band ratios. This finding is supported by that result that the yellow/green ratio derived the shallow depths in the reef flat area as 0-2 feet, in agreement with the digital nautical chart.

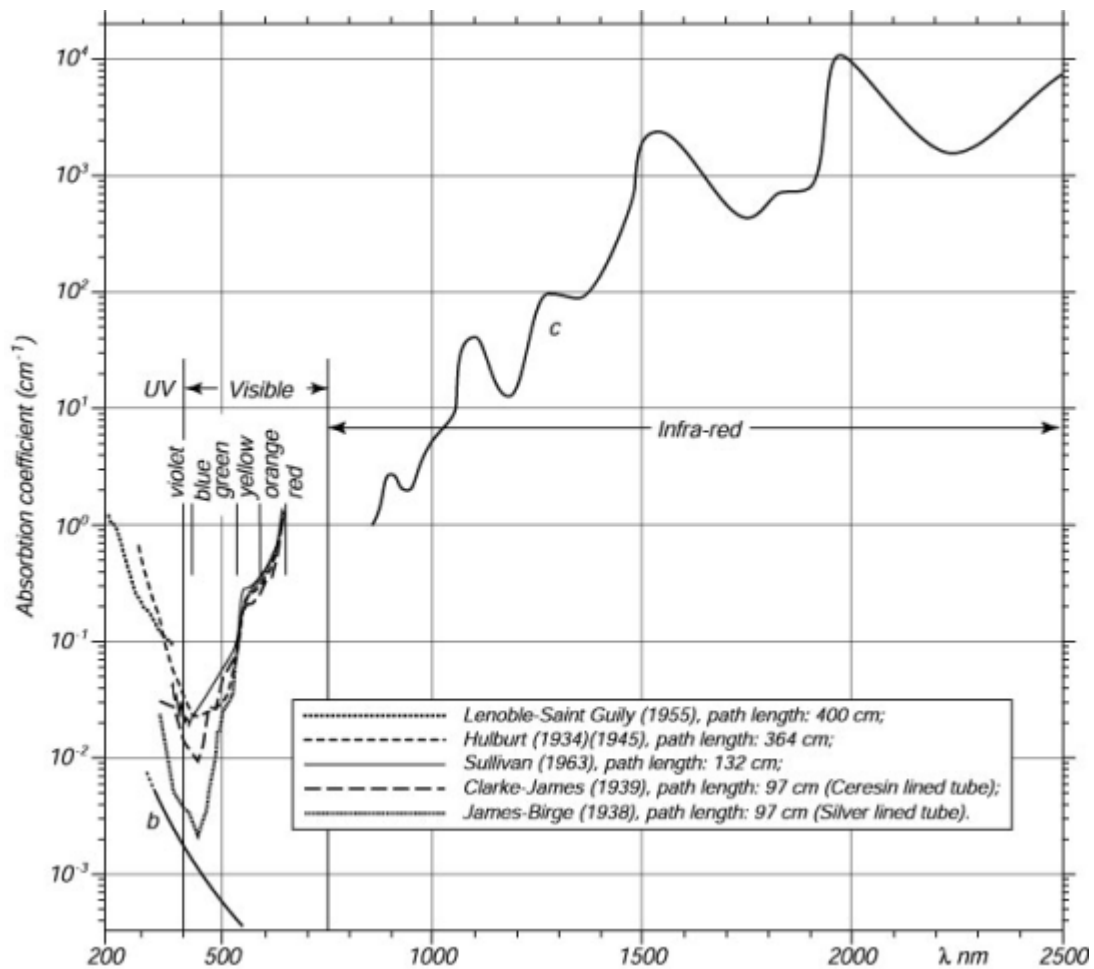


Figure 23. Attenuation rate of light with depth as a function of wavelength. (From: http://oceanworld.tamu.edu/resources/ocng_textbook/chapter06)

The difficulty of deriving accurate depth values using the green/blue ratio in shallow water is further demonstrated in Figure 21. The area along transect 2 beyond pixel 225 (depths of less than 5 ft.) shows extreme variation in derived depths, from 15 ft. to emergent. Again, the ratio appears to be sensitive to albedo, with darker substrate being derived as deeper water and extremely shallow water being derived as emergent.

The yellow/blue and the yellow/green ratios do not seem to be as sensitive to the albedo and shallow water, therefore it is difficult to determine which band (green or blue) is skewing the algorithm.

The ability to use the yellow band within the ratio algorithm greatly increases the accuracy of depth derivation in water less than 25 ft. deep. Along both transects, the depths derived with the yellow/green ratio and yellow/blue ratio agree within 5 ft. of one another. Along transect 1, the yellow/green ratio agrees very strongly with the ground truth depths extracted from the digital nautical chart in depths less than 10 ft. As the depth drops off beyond the reef crest (pixel 75, Figure 18) the yellow/blue ratio agrees very strongly with the ground truth depths while the yellow/green ratio overestimates the depth by about 5 feet. Interestingly, the green/blue ratio agrees somewhat with the yellow/blue ratio but shows significant variability from pixel to pixel. Again, this variability is likely due to albedo differences rather than depth differences. Some authors (Camacho, 2006; Siciliano, 2005) apply a filter that would smooth out this variability, but it is useful to see the raw results to demonstrate the sensitivity of the green/blue ratio to albedo compared to the yellow ratios.

The ratios using the yellow band also show similar depth derivation results along transect 2. Once again, the yellow/green band seems to overestimate the derived depths in water deeper than 10 ft. However, the difference between the two yellow ratios and the ground truth depths aren't as dramatic as those along transect 1. Additionally, it is difficult to demonstrate the improved depth derivation using the yellow/green band in water less than 10 ft. due to the lack of ground truth points. The ratios seem to follow the same pattern beyond pixel 275 along transect 2 (Figure 21) as they do in the shallow water along transect 1, but the depth is too variable and shallow (emergent to 2 ft.) to say definitively which ratio is correct.

One of the major limitations to deriving bathymetry using the ratio method is that it requires ground truth bathymetry to “tune” the parameters. The best case scenario for a study such as this one is to have access to multibeam sonar data, LIDAR bathymetry, or other data that provides very high resolution depth data. Of course, in a practical sense, the utility of using multispectral imagery to derive bathymetry is its ability to do so with

few soundings. Other studies (Camacho, 2006; Stumpf et al., 2003; Densham, 2005; Hogrefe, 2008) have demonstrated the ability to use nautical chart soundings as ground truth depths for remotely sensed bathymetric derivation. Additionally, even if high resolution depth data were available, its accuracy within 1-2 ft. is still suspect unless the survey occurred concurrently with the image acquisition. Corals grow, sand shifts, and natural and anthropogenic sources alter the bathymetry over time. Therefore, while nautical chart soundings may lack some degree of accuracy, it is debatable how much this affects the ability to derive bathymetry from remote sensing in lieu of a “better” set of ground truth data. For these reasons, this study utilizes a digital nautical chart available freely on the internet to extract ground truth depths.

VI. CONCLUSION

A number of previous studies have demonstrated the usefulness of the Stumpf et al., (2003) method to derive bathymetry using multispectral imagery. The primary limitations to this method have been its sensitivity to the albedo differences inherent in heterogeneous substrates and the difficulty in deriving shallow depths over high albedo substrates. The ability to use the yellow band in conjunction with the green and blue bands available with multispectral imagery overcomes these limitations. The Worldview-2 sensor will enable users to derive bathymetry to a higher degree of accuracy than previously possible with existing multispectral sensors.

Multispectral bathymetry mapping remains the most efficient means by which users can determine depths over large areas and remote regions with the least logistical support and cost requirements. Acquiring accurate bathymetry, especially shallow water bathymetry, will remain an important requirement for the foreseeable future. Coastal managers can use this method for any number of applications, from measuring depth changes due to storms to mapping coastal sand flow. Civilian agencies may be able to use this method to chart previously uncharted regions, or to improve out-of-date nautical charts. Military agencies, in particular, may find this method useful for mapping bathymetry in denied areas.

Several opportunities for improvement on this study exist. The most pressing need is for more accurate ground truth data. These ground truth data can be compared to the values derived in this study to determine their validity to a much higher degree of accuracy. If a bathymetric survey can be conducted in conjunction with, or near the same time as, an AVIRIS overflight, the algorithm parameters can be tuned much more closely to the actual depths and the resultant bathymetry compared to that derived in this study. In particular, the difference of the depths derived with the yellow/green ratio compared to the yellow/blue ratio needs to be explored further. In order to do this, very accurate bathymetry will be required in depths less than 10 ft. Again, these ground truth data will need to be collected nearly concurrently with the remotely sensed imagery to minimize

temporal variability in the substrate. Finally, when the actual Worldview-2 sensor comes on line, this study could be repeated to determine what benefits the yellow band (and other additional bands) provide for depth derivation.

APPENDIX A: AVIRIS REGRESSIONS

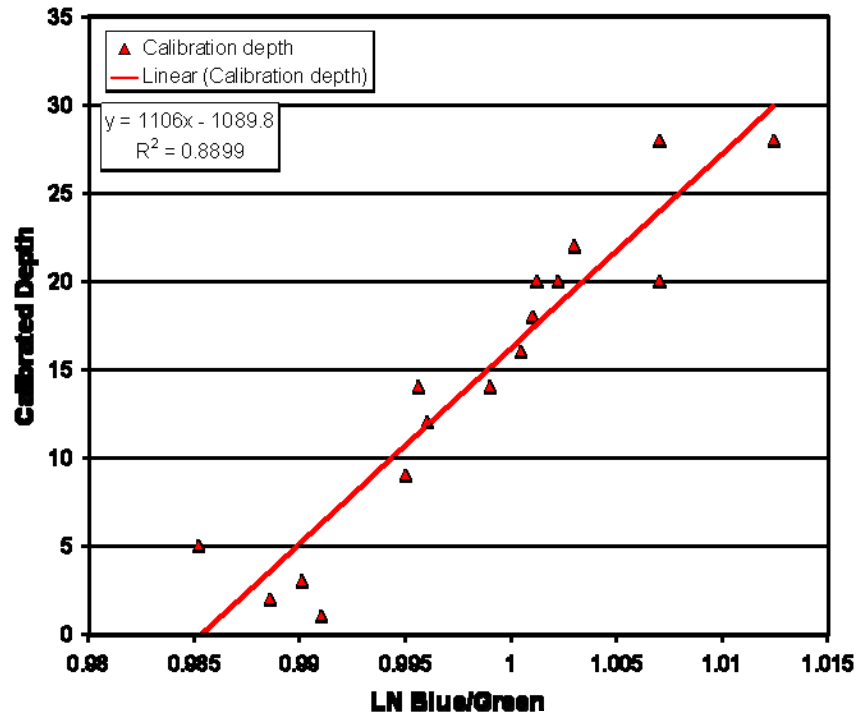


Figure 24. AVIRIS reef regression to calibrate relative bathymetry to absolute bathymetry using the green/blue ratio. Points represent ground truth points extracted from the digital nautical chart (y axis) and the value of the same point on the AVIRIS image derived from the blue/green ratio relative bathymetry regression (x axis).

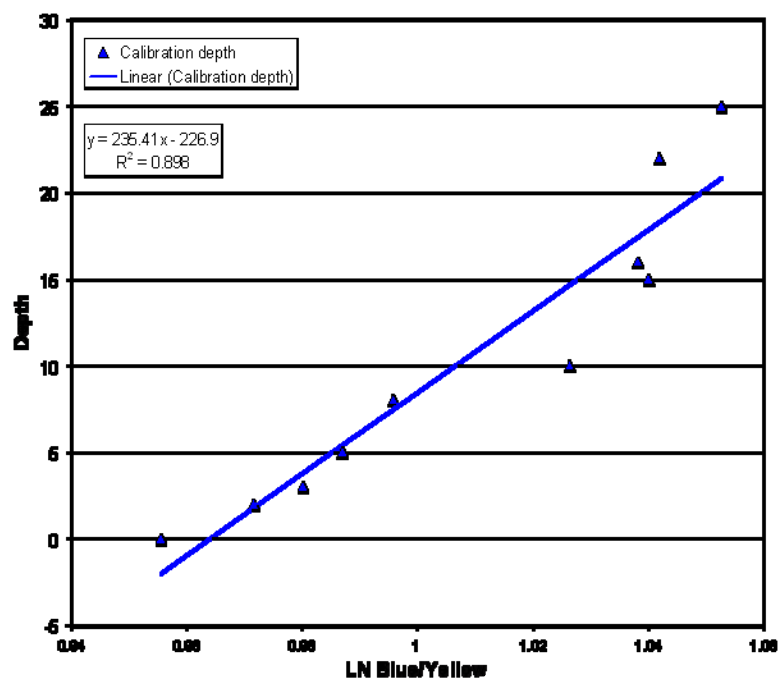


Figure 25. AVIRIS reef regression to calibrate relative bathymetry to absolute bathymetry using the yellow/blue ratio. Points represent ground truth points extracted from the digital nautical chart (y axis) and the value of the same point on the AVIRIS image derived from the yellow/blue ratio relative bathymetry regression (x axis).

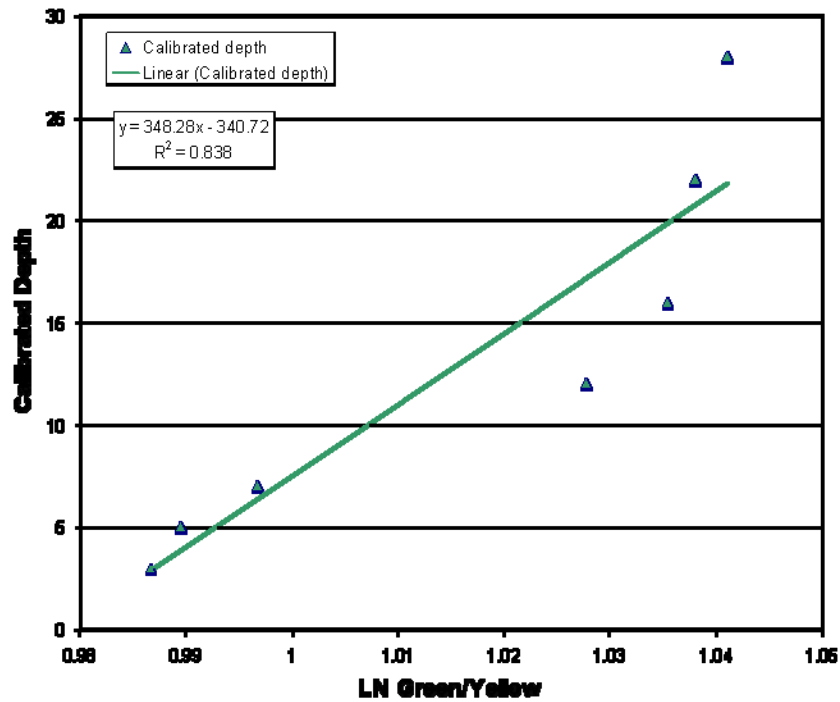


Figure 26. AVIRIS reef regression to calibrate relative bathymetry to absolute bathymetry using the yellow/green ratio. Points represent ground truth points extracted from the digital nautical chart (y axis) and the value of the same point on the AVIRIS image derived from the yellow/green ratio relative bathymetry regression (x axis).

THIS PAGE INTENTIONALLY LEFT BLANK

APPENDIX B: QUICKBIRD REGRESSION

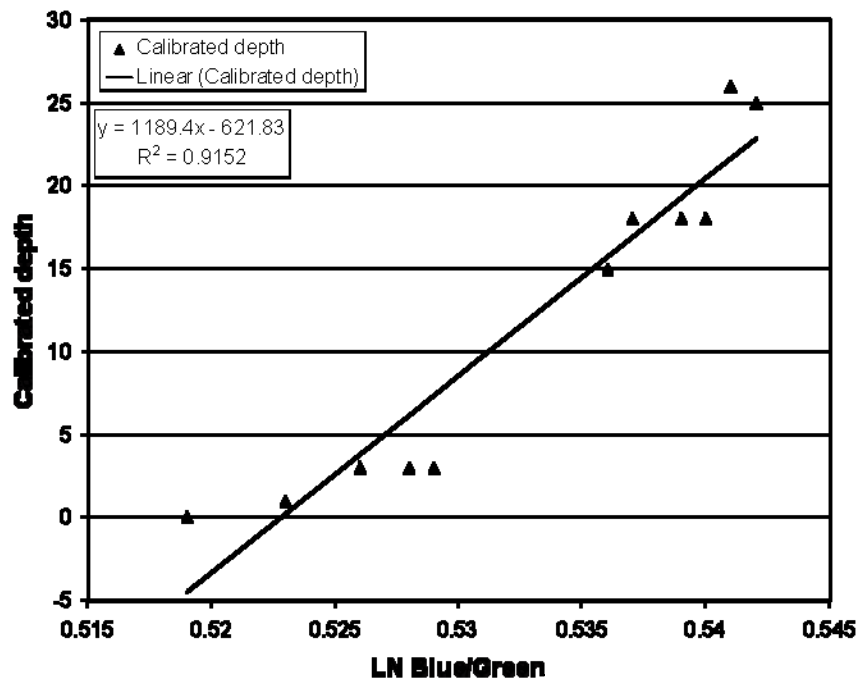


Figure 27. Quickbird reef regression to calibrate relative bathymetry to absolute bathymetry using the green/blue ratio. Blue points represent ground truth points extracted from the digital nautical chart (y axis) and the value of the same point on the Quickbird image derived from the green/blue ratio relative bathymetry regression (x axis).

THIS PAGE INTENTIONALLY LEFT BLANK

LIST OF REFERENCES

- Benny, A. H., and G. J. Dawson, 1983: Satellite imagery as an aid to bathymetric charting of the Red Sea. *The Cartographic Journal*, **20** (1), 5-16.
- Bowditch, N., 1995: *The American Practical Navigator*. National Imagery and Mapping Agency.
- Camacho, M. A., 2006: Depth analysis of Midway Atoll using Quickbird multi-spectral imaging over variable substrates. M. S. Thesis, Dept. of Space Systems Operations, the Naval Postgraduate School.
- Clark, R. E., 2005: Naval satellite bathymetry: A performance assessment. M. S. Thesis, Dept. of Meteorology, the Naval Postgraduate School.
- Densham, M. P. J., 2005: Bathymetric mapping with Quickbird data. M. S. Thesis, Dept. of Oceanography, the Naval Postgraduate School.
- Goodman, J. A., Z. Lee, and S. L. Ustin, 2008: Influence of atmospheric and sea-surface corrections on retrieval of bottom depth and reflectance using a semi-analytical model: a case study from Kaneohe Bay, Hawaii. *Applied Optics*, **47** (28), F1-F11.
- Green, E. P., P. J. Mumby, A. J. Edwards, and C. D. Clark, 2000: *Remote Sensing Handbook for Tropical Coastal Management*. UNESCO.
- Hogrefe, K. R., 2008: Derivation of near-shore bathymetry from multispectral satellite imagery used in a coastal model for the topographic analysis of human influence on coral reefs. M. S. Thesis, Dept. of Geography, Oregon State University.
- Jupp, D. L. P., 1988: Background and extensions to depth of penetration (DOP) mapping in shallow coastal waters. Proceedings of the Symposium on Remote Sensing of the Coastal Zone, Queensland, September 1988, IV2.1-IV2.29.
- Kunzig, R., 2000: *Mapping the Deep: The Extraordinary Story of Ocean Science*. W. W. Norton & Company.
- Lyzenga, D. R., 1978: Passive remote sensing techniques for mapping water depth and bottom features. *Applied Optics*, **17** (3), 379-383.
- Marsigli, L., 1725: *Histoire Physique de la Mer*. Doubleday and Company, Inc.
- Mumby, P. J., E. P. Green, A. J. Edwards, and C. D. Clark, 1999: The cost-effectiveness of remote sensing for tropical coastal resources assessment and management. *Journal of Environmental Management*, **55**, 157-166.

- Mustard, J. F., M. I. Staid, and W. J. Fripp, 2001: A semianalytical approach to the calibration of AVIRIS data to reflectance over water application in a temperate estuary. *Remote Sensing of Environment*, **75**, 335-349.
- NOAA, 2006: Nautical Charts. Retrieved November 4, 2008 from the World Wide Web: (<http://celebrating200years.noaa.gov/datasets/charts/welcome.html#pro>)
- Olsen, R. C., 2007: *Remote Sensing From Air and Space*. SPIE.
- Siciliano, D., 2005: Latitudinal limits to coral reef accretion: testing the Darwin point hypothesis at Kure Atoll, Northwestern Hawaiian Islands, using new evidence from high resolution remote sensing and in-situ data. Doctoral Dissertation, the University of California at Santa Cruz.
- Stumpf, R. P., K. Holderied, and M. Sinclair, 2003: Determination of water depth with high-resolution satellite imagery over variable bottom types. *Limnology and Oceanography*, **48** (1), 547-556.

INITIAL DISTRIBUTION LIST

1. Defense Technical Information Center
Ft. Belvoir, Virginia
2. Dudley Knox Library
Naval Postgraduate School
Monterey, California
3. Ernie Reith
National Geospatial-Intelligence Agency
Bethesda, Maryland
4. Neil Anderson
DigitalGlobe
Longmont, Colorado
5. Walter Scott
DigitalGlobe
Longmont, Colorado